The SNO/SOH TMT strategy for combinatorial analysis of reversible cysteine oxidations

Wojdyla, Katarzyna Iwona; Williamson, James; Roepstorff, Peter; Rogowska-Wrzesinska, Adelina

Published in:
Journal of Proteomics

DOI:
10.1016/j.jprot.2014.10.015

Publication date:
2015

JOURNAL OF PROTEOMICS 113 (2015) 415–434

Available online at www.sciencedirect.com

ScienceDirect

www.elsevier.com/locate/jprot

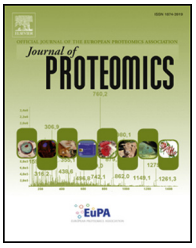

The SNO/SOH TMT strategy for combinatorial analysis of reversible cysteine oxidations

Katarzyna Wojdyla[1], *James Williamson*[1], *Peter Roepstorff*, *Adelina Rogowska-Wrzesinska*[*]

Protein Research Group, Department of Biochemistry and Molecular Biology, University of Southern Denmark, Denmark

ARTICLE INFO

Article history:
Received 23 May 2014
Accepted 18 October 2014

Keywords:
S-nitrosylation
S-sulfenylation
Site occupancy
Quantitative proteomics
Escherichia coli
Oxidative stress

ABSTRACT

Redox homeostasis is essential for normal function of cells and redox imbalance has been recognised as a pathogenic factor of numerous human diseases. Oxidative modifications of cysteine thiols modulate function of many proteins, mediate signalling, and fine-tune transcriptional and metabolic processes. In this study we present the SNO/SOH TMT strategy, which enables simultaneous analysis of two different types of cysteine modification: S-nitrosylation (SNO) and S-sulfenylation (SOH). The method facilitates quantitation of modification changes corrected by changes in protein abundance levels and estimation of relative modification site occupancy in a single nLC-MSMS run. The approach was evaluated *in vivo* using an *Escherichia coli* based model of mild oxidative stress. Bacteria were grown anaerobically on fumarate or nitrate. Short-term treatment with sub-millimolar levels of hydrogen peroxide was used to induce SOH. We have identified and quantified 114 SNO and SOH modified peptides. In many instances SNO and SOH occupy the same site, suggesting an association between them. High site occupancy does not equate to a site of modification which responds to redox imbalance. The SNO/SOH TMT strategy is a viable alternative to existing methods for cysteine oxidation analysis and provides new features that will facilitate our understanding of the interplay between SNO and SOH.

Biological significance
SNO/SOH TMT strategy outperforms other available strategies for cysteine oxidation analysis. It provides quantitative profiling of S-nitrosylation and S-sulfenylation changes simultaneously in two experimental conditions. It allows correction of modification levels by protein abundance changes and determination of relative modification site occupancy — all in a single nLC-MSMS experiment based on commercially available reagents. The method has proven precise and sensitive enough to detect and quantify endogenous levels of oxidative stress on proteome-wide scale.

1. Introduction

Cellular thiol redox state is a crucial mediator of multiple metabolic, signalling, and transcriptional processes in cells. Balance between oxidising and reducing conditions is essential for the normal function and survival of cells. Oxidative stress has been recognised as pathogenic and etiological factor of numerous human diseases, including cancer, diabetes, atherosclerosis,

[*] *Corresponding author at:* Campusvej 55, 5230 Odense M, Denmark. Tel.: +45 6550 2351.
E-mail address: adelinar@bmb.sdu.dk (A. Rogowska-Wrzesinska).
[1] Equal contribution.

http://dx.doi.org/10.1016/j.jprot.2014.10.015
1874-3919/

cardiovascular and neurodegenerative diseases [1]. It is also involved in physiological ageing and degenerative processes that occur in age-related diseases. Protein thiols, due to their ability to be reversibly oxidised, are recognised as key components involved in the maintenance of redox homeostasis [2]. There are 7 recognised oxidative modifications of cysteine, 5 of which are reversible [2]. Among these, S-nitrosylation (SNO) and S-sulfenylation (SOH) play a significant role in regulating cellular signalling in response to redox imbalance. SNO is a covalent addition of nitroso group onto the reduced thiol of cysteine's side chain. Endogenous sources of nitroso group are for instance, the nitric oxide synthase (NOS) family of enzymes [3]. There are representatives of the NOS family in almost every cell type (neuronal nNOS/NOS1, endothelial eNOS/NOS3, inducible/Ca^{2+}-independent iNOS/NOS2) [3]. Indirectly, SNO may also occur *via* contact with existing nitrosylated proteins that act as nitroso group donors, in a process termed trans-nitrosylation [4]. SOH is an oxidation of the cysteine sulfhydryl to sulfenic acid. The major inducer of SOH is hydrogen peroxide (H_2O_2), which is generated in the cell *e.g.*, as a product of superoxide dismutase catalytic activity [5].

SNO and SOH do not occur equally over all cysteine residues due to the variable electronegativity of cysteine in biological systems. This, combined with their transient nature makes them excellent signalling mediators [1]. For example, in *Escherichia coli* grown anaerobically on nitrate, SNO of OxyR initiates a signalling cascade activating mechanisms protecting against endogenous nitrosative stress [6]. Antioxidant buffering capacity is also an important function of SNO. Elevated levels of SNO during ischemic preconditioning prevent build-up of irreversible protein oxidations helping to guard against irreversible oxidative damage during reperfusion [4]. SOH is known to function as a transient intermediate in the formation of more stable cysteine oxidation products [7] and it is an indicator of oxidant-sensitive cysteines and potentially also of severe oxidative damage [8]. It is implicated in redox regulation of transcription factors [9]. Protein SOH can modify the activity of enzymes [10,11] and act as an initiator of disulfide bond formation [12].

For effective analysis of SNO and SOH selective labelling and enrichment are required [13]. A number of methods for analysis of cysteine oxidation exist, each with certain advantages and limitations, as reviewed in [2]. The majority of strategies used in the analysis of protein SNO, are variations of the biotin switch technique [14]. The most advanced of these provide precise localisation of modification site and its relative abundance [15–17]. Biotin switch has also been adapted for analysis of cysteine SOH [18]. However, dimedone labelling is more widespread [19,20]. Recently, new cell-permeable analogues of dimedone have been developed which significantly shortens the time for sulfenic acid selective capture thus minimising artifactual results [21,22].

Despite dynamic advances in molecular biology and mass spectrometry-based strategies for analysis of cysteine redox proteomes there remain several challenges. The majority of current methods provide quantitative information, yet, correction of modification levels by protein abundance changes is still a rare practise. In fact there are only few existing methods which either inherently correct observed modification levels in such a way [15], or with additional workload provide such correction [23–25]. However, all of these approaches use non-isobaric isotopic labels which suffer from low throughput due to increased sample complexity, limited dynamic range of quantitation and typically can target only 2 samples/conditions due to isotopic limitations. An additional layer of quantitative information relevant for determining the functional importance of a given modification is site occupancy [26]. Again, only rarely and at the expense of additional analytical steps has this been addressed [27,28]. Finally, few methods exist that target multiple cysteine oxoforms. Attempts have been made to target the SNO and a pool of all reversibly oxidised cysteines in parallel [29]. However, further development of such strategies targeting individual modifications simultaneously is important to decode potential cross-talk between different cysteine oxoforms.

In addition to the limitations of existing methods the majority of studies investigating cysteine oxidative modifications use *in vitro* models where oxidation is induced chemically, for example by treatment with S-nitrosoglutathione (GSNO) [30,31]. Such models do not reflect physiological levels of oxidative modifications. Additionally, they are often performed outside cellular environment and in denaturing conditions, which neglects the role of protein structure in the susceptibility of cysteine to oxidation.

Here we present an analytical strategy which provides quantitative analysis of cysteine SNO and SOH simultaneously including precise assignment of modification site. The method inherently corrects for protein abundance changes and permits determination of relative site occupancy of both modifications. To achieve this we make use of Iodoacetyl Tandem Mass Tags (iodoTMT™) which are a variant of the popular amine reactive TMT™ isobaric labels. Replacement of the amine reactive group with a thiol reactive iodoacetyl moiety allows for quantitative analysis of cysteine subproteomes by tandem mass spectrometry [32]. Enrichment or immunoassay based detection of iodoTMT™-containing peptides and proteins is achieved by the application of an anti-TMT™ antibody. As with their amine counterpart, isobaric iodoTMT™ tags allow for concurrent analysis of up to six samples [32]. In the presented configuration, our SNO/SOH TMT method allows analysis of two treatment groups in one experiment.

SNO/SOH TMT was developed and optimised to target near physiological levels of oxidative stress and to characterise proteins modified in native conditions. To test the applicability of the method to analysis of complex biological samples we have used SNO/SOH TMT strategy to analyse the thiol redox proteome of *E. coli* under mild oxidative stress induced *in vivo*. Our model was built upon previous works with minor alterations [6]. Induction of SNO was achieved by anaerobic growth in minimal media supplemented with nitrate, whereas fumarate was used in the control group. SOH was induced by brief in-culture stimulation with hydrogen peroxide (H_2O_2).

We show that the SNO/SOH TMT strategy provides robust and reproducible method for identification of the modification site and quantification of the relative abundance of SNO and SOH in proteins. Combined with anti-TMT™ enrichment it is sensitive enough to measure the endogenous levels of thiol modifications. Our results indicate that SNO and SOH coexist on several cysteine residues and only few of the modified residues change between low and mild oxidative

stress conditions. The approach presented expands out tool-box for redox proteome analysis and opens up new possibilities for studying the interdependence of different cysteine oxoforms. We emphasise that although SNO/SOH TMT is a powerful methodology for screening of SNO and SOH alterations in response to changes in ROS/RNS levels, the information it provides should be evaluated further with alternative analytical strategies in order to reveal their true biological importance.

2. Materials and methods

2.1. Materials

Anaerogen, iodoTMT™ tags, immobilised and unbound anti-TMT™ antibody, Tris-buffered saline (TBS), tris(2-carboxyethyl) phosphine (TCEP), TMT elution buffer, Pierce Screw Cup Spin Columns Zeba Spin desalting columns and BCA assay were from Thermo Scientific. The remaining chemicals were from Sigma Aldrich unless stated otherwise. All solvents were of analytical or higher grade.

2.2. Methods

For all reagents, final concentrations are reported, unless started otherwise. All steps from oxidation induction to quenching after iodoTMT™ labelling were performed under minimal light exposure.

2.2.1. Cultivation of E. coli, in vivo oxidation

A single colony of *E. coli* K-12 was inoculated from LB agar plate to 10 ml LB liquid medium for overnight growth at 37 °C with shaking. Overnight cultures were recovered by centrifugation and washed in MOPS minimal media once before making a 4% (v/v) inoculation into 50 ml MOPS minimal media [33] supplemented with 100 mM disodium fumarate (control, n = 3 independent biological replicates) or 100 mM sodium nitrate (stressed, n = 3). Flasks were transferred to 2.5 l anaerobic jars together with AnaeroGen and Anaerotest® (Merck, Millipore). Bacteria were grown in the dark for 7 h at 37 °C with gentle agitation. 100 μM H_2O_2 was added to the stressed group 5 min prior to cell harvest. Cells were collected by centrifugation (4500 ×*g*, 20 min, 4 °C) and washed twice with ice cold phosphate buffered saline (PBS), pH 7.4. Finally cell pellets were resuspended in lysis/blocking buffer containing 150 mM HEPES, pH 7.3, 1 mM EDTA, 0.1 mM neocuproine, 2% SDS, 50 mM MMTS (S-Methyl methanethiosulfonate). Cells obtained from 50 ml of cultures at OD_{600} = 0.7 were lysed in 4 ml of lysis/blocking buffer by applying 5 rounds of 10 s on/off sonication cycles at an amplitude of 25% in a tip sonicator (Q500, Qsonica). Cell lysates were incubated for 30 min at room temperature (RT) with gentle agitation, precipitated with 10 volumes of ice cold acetone for 1 h at −20 °C and centrifuged (4500 ×*g*, 20 min, 4 °C). Protein pellets were washed twice with ice cold acetone, using a tip probe sonicator to disrupt the pellets between washes. Washed pellets were resuspended in AENS buffer (50 mM ammonium bicarbonate, pH 8.0, 1 mM EDTA, 0.1 mM neocuproine, 2% SDS). Protein concentration was measured using BCA assay.

2.2.2 . iodoTMT™-6plex labelling

IodoTMT™ 6plex reagents were used in reductive alkylation of both control and stressed samples. For total cysteine labelling, 100 μg of protein extracts (1 μg/μl) was reduced with 10 mM TCEP in AENS buffer for 1 h at 56 °C. TCEP was then removed using Zeba Spin desalting columns exchanging buffer for AENS buffer without TCEP, following the manufacturer's instructions. Reduced samples were alkylated with 5 mM iodoTMT™-126 (control) and iodoTMT™-127 (stressed). For SNO, 1 mg of each sample (2 μg/μl) was reduced with 20 mM sodium ascorbate and alkylated with 0.9 mM iodoTMT™-128 (control) and iodoTMT™-129 (stressed). For SOH, 1 mg of each sample (2 μg/μl) was reduced with 10 mM sodium (meta) arsenite and alkylated with 0.9 mM iodoTMT™-130 (control), iodoTMT™-131 (stressed). For all the samples, iodoTMT™ labelling was carried out for 2 h at 37 °C with shaking. Reactions were quenched by adding 500 mM dithiothreitol (DTT) and 15 min incubation. An aliquot of each sample (4 μg) was saved for western blot analysis before combining all samples. Samples were pooled using the following scheme: 1:10:10 of total cysteines:SNO:SOH and precipitated with 10 volumes of ice cold acetone overnight at −20 °C. Pellets were washed three times with ice cold acetone/methanol (50% v/v) to remove excess iodoTMT™ reagents.

2.2.3. Reduction, alkylation, enzymatic digestion and peptide desalting

Final protein pellets were resuspended in digestion buffer (50 mM ammonium bicarbonate, pH 8.0, 8 M urea). Samples were reduced with 20 mM DTT for 45 min at RT and alkylated with 55 mM iodoacetamide (IAA) for 30 min at RT in the dark. Proteins were digested with lysyl endopeptidase (Wako Pure Chemical Industries, Ltd.) for 3 h at 30 °C with shaking. Next, samples were diluted with 50 mM ammonium bicarbonate to reduce urea concentration below 2 M, before trypsin was added (1:50, enzyme to protein ratio) for overnight digestion at 37 °C with shaking.

Peptide solution after digestion was acidified with trifluoroacetic acid (TFA, 0.5%) and desalted using HLB cartridge (Oasis, Waters). Briefly, HLB cartridge was washed with methanol, acetonitrile (ACN) and 80% ACN, 0.1% TFA (1 ml each) and equilibrated with 0.1% TFA (3 × 1 ml). Peptides were loaded on the cartridge 5 times. Washing was 0.1% TFA (5 × 1 ml) followed by elution of bound peptides with 80% ACN, 0.1% TFA (1 ml). Eluates were vacuum dried and resuspended in Tris-buffered saline (TBS), pH 7.0. A small aliquot was taken for amino acid analysis on a Biochrom 30 (Biochrom Ltd., UK) to determine peptide quantities prior to anti-TMT™ enrichment.

2.2.4. Anti-TMT™ enrichment and sample clean-up

Approximately 2 mg of the iodoTMT™ 6plex sample was enriched on anti-TMT™ columns. The amount of anti-TMT™ resin was calculated from the following equation: resin slurry [μl] = 142.858 x sample amount [mg]. Samples were incubated with anti-TMT™ resin in Pierce Screw Cap Spin Columns for 2 h at RT with end-over-end shaking. For all subsequent steps, resin was incubated with each solution for 10 min as described above. Washes were: 2 M urea in TBS (2 column volumes) followed by 0.1% SDC in TBS and TBS only (3 column

volumes each). iodoTMT™-containing peptides were eluted from the resin with 4 column volumes of TMT elution buffer. Eluate fractions were acidified with TFA (0.5%), centrifuged to pellet any residual SDC (20 000 ×*g*, 5 min, RT), removed to a fresh tube and vacuum dried. Samples after anti-TMT™ enrichment were desalted on in-house made micro-columns packed with reverse phase material POROS 20R2/R3 as previously described [34,35].

2.2.5. HILIC fractionation

Portions of iodoTMT™-6plex labelled samples (20 μg) were fractionated by hydrophilic interaction chromatography (HILIC) using off-line Agilent 1200 HPLC equipped with automatic fraction collector. Samples were separated on in-house made HILIC microcolumn (320 μm ID × 15 cm packed with TSKgel Amide 80 resin (Tosoh Bioscience)) at a flow rate of 6 μl/min, in linear, 8 min gradient from 95 to 60% B. Solvent A was 0.1% TFA, solvent B was 90% ACN, 0.1% TFA. Eluted peptides were automatically collected at 1 min fractions into a 96 well plate.

2.2.6. nLC-MSMS data acquisition

nLC-MSMS data were acquired on a Dionex UltiMate™ 3000 Rapid Separation UHPLC interfaced *via* an EASY-Spray™ nano electrospray source to Q-Exactive™ Plus mass spectrometer (Thermo Scientific). The trapping column was 100 μm ID, 2 cm long, packed with 5 μm Reverse Phase C18 material (Reprosil, Dr Maisch, Germany). Analytical column was a Thermo Scientific EASY-Spray™ column of 75 μm ID, 50 cm long, packed with 2 μm C18 particles. Loading solvent was 0.1% TFA, analytical solvents A and B were 0.1% formic acid (FA) and 0.1% FA in ACN. All separations were carried out at 40 °C. Samples were resuspended in 1% TFA, 5% DMSO and loaded onto the trap column at 10 μl/min for 5 min. Peptides were eluted onto and separated over the analytical column with the linear gradient of solvent B (2–35%) for 90 min. 2.1 kV voltage was applied for electrospray. The quadrupole isolation width was set to 2 m/z. MS1 scans in the m/z range 300–1200 were acquired in the Orbitrap with 70 000 resolution at an AGC target of 1E6 and maximum injection time of 120 ms. AGC target and maximum injection time for MS2 were 2E4 and 60 ms, respectively. Tandem mass spectra were acquired in data-dependent manner with top 12 most intense ions per MS1 scan selected for fragmentation at a threshold of 10 000 counts. Dynamic exclusion was set to 45 s. Normalised collision energy (NCE) was 34 and fragment ions were detected from 110 m/z at 17 500 resolution.

2.2.7. Database search

MS data were searched against the Uniprot Reference *E. coli* proteome (4303 entries, July 13th 2012) with common contaminants from GPM appended [36] using in-house Mascot server from within Proteome Discoverer version 1.4. The following search parameters were used: enzyme — trypsin, 2 missed cleavages, precursor mass tolerance — 10 ppm and fragment mass tolerance — 20 mmu; variable modifications were — iodoTMT™ (Cys), carbamidomethylation (Cys) and oxidation (Met). Mascot Percolator was used to estimate Peptide-Spectrum Match False Discovery Rate and only peptides with a percolator q-score ≤ 0.01 were taken forward for analysis. The reporter ion quantifier node of Proteome Discoverer set to a 20 mmu tolerance, using the most confident centroid was applied to extract reporter ion intensities for TMT quantification. Default protein grouping options were applied.

2.2.8. Normalisation and significance analysis

Ratios of respective reporter ion intensities (127/126, 129/128 and 131/130) were log(2) transformed and normalised to the median value. Normalised ratios for SNO (129/128) and SOH (131/130) were corrected for the respective total cysteine ratios (127/126). The significance threshold — two times standard deviation (2 sigma) was then calculated for each of the normalised and corrected ratios of modifications. Peptides with log(2) ratios ±2 sigma were considered of highest biological significance.

2.2.9. Label-free quantitative proteomics

E. coli were grown anaerobically as described above. Cells were collected by centrifugation (4500 ×*g*, 20 min, 4 °C) and washed twice with ice cold PBS. Final cell pellets were resuspended in lysis buffer (20 mM Triethylammonium bicarbonate (TEAB) pH 8.0, 2% SDS) and lysed as above. Protein concentration was determined by BCA assay. Samples were digested on-filter with MS-compatible detergent sodium deoxycholate (SDC) [37]. Briefly, protein samples were loaded onto ultrafiltration devices (30 kDa Vivacon, Vivaproducts, Inc.) and washed first with urea to remove SDS and then with SDC to remove urea and provide a denaturing environment for digestion. Reduction (DTT) and alkylation (IAA) were performed on-filter prior to digestion with trypsin as described before [37]. Peptides were recovered by centrifugation and SDC was removed by precipitation with TFA and phase transfer into ethyl acetate as described before [38].

nLC-MSMS analysis and database search were performed essentially as above, with few exceptions. For MS2, NCE was 28 and fragment ions were detected relative to the precursor's m/z. In database search, cysteine carbamidomethylation was used as fixed and methionine oxidation as variable modification. Quantitative information from label-free experiments was retrieved from nLC-MSMS data using chromatographic alignment feature within Progenesis LC-MS (Nonlinear Dynamics). Automatic reference selection, run alignment and peak picking were used to align all acquired spectra. Search results from Proteome Discoverer were imported to identify aligned features. Significance analysis was performed using the built in ANOVA test. Proteins with at least 2 quantified peptides and ANOVA significance value $p \leq 0.05$ were considered significant.

2.2.10. In vitro oxidation and western blot analysis

A single colony of *E. coli* was inoculated from an LB agar plate into 20 ml LB liquid media and grown overnight to stationary phase before harvesting by centrifugation. Cell pellets were resuspended in HES buffer (150 mM HEPES, 1 mM EDTA, 2% SDS) and lysed by sonication as described above. Protein concentration was measured by BCA assay. 4 mg of protein lysate was used for *in vitro* oxidation and subsequent analysis. A schematic outline of the experiment is presented in Fig. S1.

S-nitrosoglutathione (GSNO) was used to induce SNO (200 μM GSNO for 30 min at RT). To induce SOH, protein

lysates were treated with 100 μM hydrogen peroxide for 15 min at 37 °C. Oxidised samples were immediately precipitated with 10 volumes of ice cold acetone, for 1 h at −20 °C. Protein pellets were washed twice with acetone and resuspended in lysis/blocking buffer. All steps from free thiol blocking until quenching after iodoTMT™ labelling were essentially as described above, with minor changes. 25 μg of protein lysate (2 μg/μl in AENS buffer) was used for labelling with iodoTMT™-zero. In addition to SNO and SOH analysis, MMTS blocking efficiency was tested. Here samples were directly incubated with 0.9 mM iodoTMT™-zero. All labelled and quenched samples were denatured in Bolt® LDS Sample Buffer with 50 mM DTT for 10 min at 70 °C. For SDS-PAGE Novex®Bolt® (Life Technologies) gel electrophoresis system was used following the manufacturer's instructions. 4 μg of each sample was loaded on a gel and separated in NuPAGE® MES SDS Running Buffer for 35 min at 165 V. Proteins were electrotransferred from gel onto a PVDF membrane (Immobilon®-P, 45 μm pore size, Merck Millipore) in cold Towbin buffer for 20 min at 18 V using semidry-western blot system (Trans-Blot® SD, Semi-Dry Transfer Cell, Bio-Rad). Membranes were incubated in blocking buffer (5% non-fat milk powder in TBS with 0.1% (v/v) Tween 20 — TBST) overnight at 4 °C with shaking. Primary antibody (anti-TMT ™ antibody; 1:5000 in blocking buffer) incubation was 1 h at RT with shaking, followed by 3 × 10 min washes in TBST. Secondary antibody (Anti-mouse IgG2b from Rabbit Peroxidase Conjugated, Rockland Immunochemicals; 1:10 000) incubation was 1 h at RT with shaking, followed by 3 × 10 min washes in TBST. For development peroxidase substrate (Luminata™ Forte, Merck Millipore) was incubated for 2 min. The chemiluminescent signal was captured using BioSpectrum® 2D Imaging System (Ultra-Violet Products Ltd). Density analysis was performed using Image Studio™ Lite version 3.1 (LI-COR® Biosciences) as previously described [39].

3. Results

3.1. SNO/SOH TMT — method for simultaneous analysis of SNO and SOH

We have developed and tested a proteomics-based strategy for simultaneous detection and quantitation of two reversible cysteine modifications, SNO and SOH. The basic principles of the strategy are presented in Fig. 1. SNO/SOH TMT strategy is based on alkylation with Iodoacetyl Tandem Mass Tags (iodoTMT™ tags) for labelling of reduced cysteines (SH) and TMT specific antibody for enrichment of iodoTMT™ labelled peptides.

The method consists of five components: 1) cell lysis and reversible blocking of free SH groups with MMTS; 2) differential reduction of "total" cysteines, S-nitrosylated cysteines and S-sulfenylated cysteines with TCEP, sodium ascorbate and sodium arsenite respectively followed by iodoTMT™ alkylation; "total" cysteines refers to all cysteines that are/can be reduced to sulfhydryl groups, this includes free cysteines and all DTT/TCEP reducible cysteine modifications including disulfides (S-S), SNO and SOH 3) reduction and alkylation of pooled samples followed by proteolytic digestion; 4) enrichment of iodoTMT™-containing peptides using TMT specific antibody; and 5) analysis of peptide fractions by nano liquid chromatography coupled to tandem mass spectrometry (nLC-MSMS). The experimental conditions used in this study have been adapted from the iodoTMT™ supplier instructions [40] and tested for suitability in the described workflow. Table 1 and Fig. S2 summarise the different steps of the method.

3.1.1. Blocking of free thiols

Free thiol blocking is critical. Any failure at this step will artifactually increase the final cysteine oxidation readouts. For the *E. coli* protein extracts used in this study we have determined that 4 ml of lysis/blocking buffer was sufficient to block sulfhydryl groups from ~3.5×10^{10} *E. coli* cells obtained from 50 ml culture at OD_{600} of 0.7. The final concentration of MMTS was 50 mM, which roughly corresponds to 33 nmol MMTS per 1 μg protein. The efficiency of MMTS blocking was assessed by western blot analysis (Fig. 2A and Fig. S3A). Additionally we have observed that simultaneous cell lysis and MMTS blocking as opposed to sequential cell lysis and MMTS blocking gave the most complete and reproducible results (data not shown). Despite extensive optimisation, MMTS blocking was not complete and a low background signal was detected (Fig. S3A).

3.1.2. Selectivity of modification specific reductions

The concept of SNO/SOH TMT is built upon the selectivity of modification specific reductions. Based on the current literature we have chosen 20 mM ascorbate and 10 mM arsenite for selective reduction of SNO and SOH respectively [29,41]. Western blot analysis was used to test the efficiency of modification specific reductions, the outline of the experiment is presented in Fig. S1. For testing the specificity of reductions, SNO and SOH were induced *in vitro*, by direct treatment of *E. coli* lysates with GSNO and H_2O_2 respectively. Each fraction was alkylated with iodoTMT™ reagent either directly (H_2O) to test efficiency of free thiol blocking with MMTS or after ascorbate or arsenite reduction. The level of iodoTMT™ label incorporation into proteins was detected by anti-TMT™ antibody. The results are shown in Fig. 2A. As expected, the non-oxidised proteins (control) have shown an equal, relatively low signal in all reduction conditions. Proteins treated with GSNO have shown a similar low signal level for non-reduced samples (H_2O) and samples reduced with arsenite. These low levels of unspecific iodoTMT™ labelling are most likely due to incomplete blocking of free sulfhydryls with MMTS. At the same time samples treated with ascorbate, which specifically reduces SNO, have shown a 5 fold signal increase, confirming the efficient iodoTMT™ labelling of SNO modified cysteines. Proteins treated with H_2O_2 have shown a similar pattern of increased signal observed in arsenite reduced samples as compared to the control. Interestingly H_2O_2 treated samples that were subsequently reduced with ascorbate have shown a similar level of iodoTMT™ label incorporation as those reduced with arsenite indicating the presence of SNO groups. Under these particular oxidative conditions not only SOH but also SNO was increased. Although H_2O_2 was not known to induce SNO directly, elevated SNO levels in the presence of H_2O_2 have been reported previously [42]. Additionally, a recent study by Hlaing et al. clearly documents increased protein

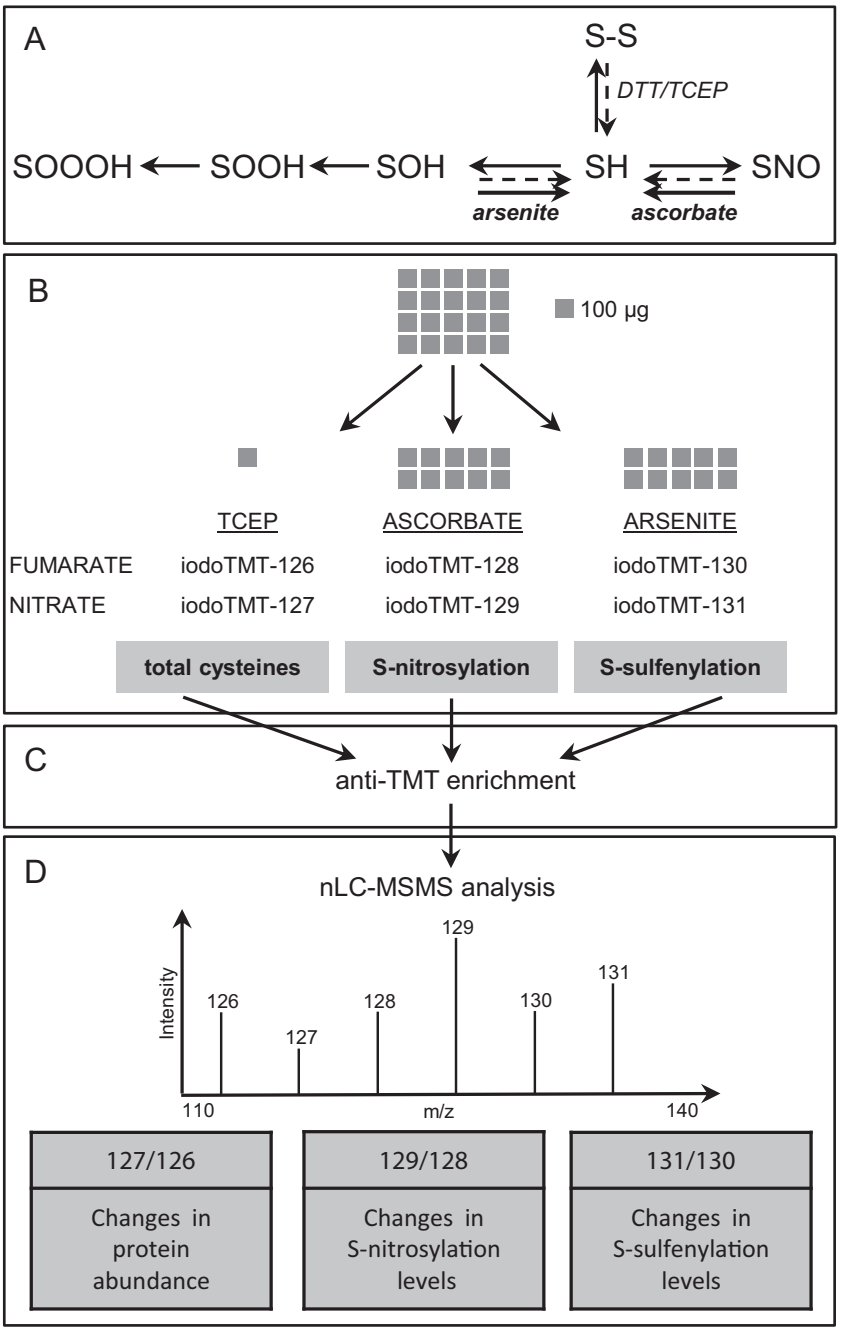

Fig. 1 – Outline of SNO/SOH TMT strategy. A. oxidative modifications of cysteine; SH — sulfhydryl group; S–S — disulfide bond; SNO — S-nitrosylation; SOH — S-sulfenylation; SOOH — sulfinic acid; SOOOH — sulfonic acid. Dashed arrows indicate non-selective reduction of all DTT/TCEP reducible modifications; bold arrows indicate modification specific reductions; B. iodoTMT™-6plex based differential alkylation of total, S-nitrosylated and S-sulfenylated cysteines in two different growth conditions (fumarate/nitrate); C. anti-TMT™ enrichment; pooled samples are enzymatically digested and iodoTMT™-containing peptides are affinity purified on immobilised antibody columns; D. quantitative nLC-MSMS analysis; reporter ion intensities in the low m/z range of MSMS spectra are used to measure relative changes in protein abundance and S-nitrosylation and S-sulfenylation levels respectively.

S-nitrosylation as a direct response to H_2O_2 treatment in serum starved mouse embryonic fibroblasts [43]. H_2O_2 may also mimic and complement the effects of nitric oxide as it has been reported for human platelets [44]. The chemistry behind such interplay remains unsolved [45]. Both modification specific reductions resulted in a higher signal than the negative control and a much lower signal than in the fully reduced control (Fig. 2A and Fig. S4).

Table 1 – Optimised conditions for SNO/SOH TMT strategy for simultaneous identification and quantitation of 3 distinctive cysteine subsets.

	Step	Final conditions used
Cell lysis and free thiol blocking	Blocking of free SH groups	50 mM MMTS[a] in lysis buffer
	Removal of MMTS excess	Acetone precipitation for 1 h at −20 °C
Differential reduction and alkylation	Total cysteine reduction	Sequential reduction (10 mM TCEP) and alkylation (5 mM iodoTMT™)
	SNO reduction	20 mM ascorbate (0.9 mM iodoTMT™)
	SOH reduction	10 mM arsenite (0.9 mM iodoTMT™)
	iodoTMT™ labelling	2 h at 37 °C
	Quenching excess iodoTMT™	500 mM DTT for 15 min at 37 °C
Multiplexing	Mixing ratio	1 (total):10 (SNO/SOH)
	Peptide quantitation	Amino acid analysis
Anti-TMT™ enrichment	Amount of anti-TMT™ resin slurry	200 μl[b]
	Incubation	2 h at RT (24 ± 1 °C)
	Washing	Sequential: urea, SDC, TBS[c]
	Elution	TMT elution buffer[d]

[a] All values refer to final concentrations of chemicals during reaction.
[b] For both total and SNO/SOH labelling resin amount was calculated based on manufacturer's recommendations.
[c] Washing buffers were: 2 M urea in TBS, 0.1% SDC in TBS and TBS only.
[d] When using TMT elution buffer triethylammonium (TEA)-containing buffers should be avoided throughout the procedure.

3.1.3. Multiplexing

The stoichiometry of SNO/SOH modified cysteines compared to the number of total cysteines is low. This is important when considering the labelling chemistry and in which ratio labelled protein is mixed. TCEP reduced protein has a high number of potential sites at which iodoTMT™ may be incorporated. Therefore it requires a relatively higher amount of iodoTMT™ label per amount of protein than for ascorbate (SNO) and arsenite (SOH) reductions. Additionally, to maintain a balance between reporter ion intensities less protein from TCEP reduction (total cysteine labelling) should be used than for either ascorbate or arsenite reduction. Based on western blot and mass spectrometry analysis we have determined that 10 times less protein for total cysteine (TCEP reduced) compared to modified (ascorbate or arsenite reduced) was appropriate (Fig. 2B and Fig. S4).

3.1.4. Enrichment of TMT labelled peptides

In the presented approach we have followed the recommendations provided by the iodoTMT™ supplier [40]. This included a wash step with sodium deoxycholate where washing with a "mass spectrometry compatible detergent" was recommended. The selectivity of the enrichment obtained ranged from 50% in samples containing high levels of iodoTMT™ labelled peptides (*e.g.* where iodoTMT™ labelling was achieved by reduction and alkylation of total cysteines or chemical induction of SNO/SOH) to 7% for samples where the levels of SNO and SOH were endogenous (induced by growth on nitrate and H_2O_2 stress).

We hypothesised that peptide pre-fractionation could replace anti-TMT™ enrichment when dealing with a low amount of starting material. We have compared hydrophilic interaction chromatography (HILIC) based fractionation of a low amount of starting material (20 μg) with anti-TMT™ enrichment of a high amount of starting material (2 mg). The experimental outline is presented in Fig. 3A. Using HILIC fractionation, we have identified 254 unique, iodoTMT™-containing peptides (n = 3 independent biological replicates, Table S1). Anti-TMT™ enrichment resulted in total of 481 unique, iodoTMT™ peptides (n = 3). The overlap between the two techniques was 23%, corresponding to 139 peptides (Fig. 3B). In order to evaluate the benefits of the enrichment strategy we have estimated the precursor areas based abundance of iodoTMT™-containing peptides identified by both methods (Fig. 3C). The results show that the abundance of iodoTMT™ containing peptides from HILIC fractionation is only 40% of respective peptides quantified by iodoTMT™ enrichment approach.

Next we sought to investigate the quantitative precision of the results obtained by the two approaches. We have plotted the log(2) ratios of SNO/SOH peptides found in both iodoTMT™ enriched and HILIC pre-fractionated samples. The average correlation from all 3 biological replicates was $R^2 = 0.749$, ±0.16 for total cysteines, $R^2 = 0.361$, ±0.16 for SNO and $R^2 = 0.204$, ±0.09 for SOH (Fig. S5). Despite the good correlation between quantitative information on total cysteines, the correlation between modifications is poor. This can be traced back to very low reporter ion intensities in the HILIC pre-fractionated samples, which were on average an order of magnitude lower, relative to anti-TMT™ enrichment (see Tables in Fig. S5). As the total cysteine reporter ions are generally more intense than for the modifications, this intensity reduction was not sufficient to compromise quantitative precision. However, in the case of SNO and SOH, the reporter ion intensities are low in the enriched samples and therefore even lower in the HILIC samples. This resulted in diminished quantitative precision.

3.2. Anaerobic growth on nitrate or fumarate induces alterations in protein abundance and oxidation levels

The presented analytical strategy was tested on *E. coli* extracts where endogenous proteins SNO and SOH were induced. This was achieved by following a previously published protocol with few alterations [6]. Briefly, to obtain low oxidative growth conditions *E. coli* were cultured anaerobically using fumarate as a terminal electron acceptor. These conditions were compared to *E. coli* cells grown in the presence of nitrate, which was expected to induce accumulation of S-nitrosylated proteins. Finally, SOH was induced by addition of H_2O_2 to the nitrate culture.

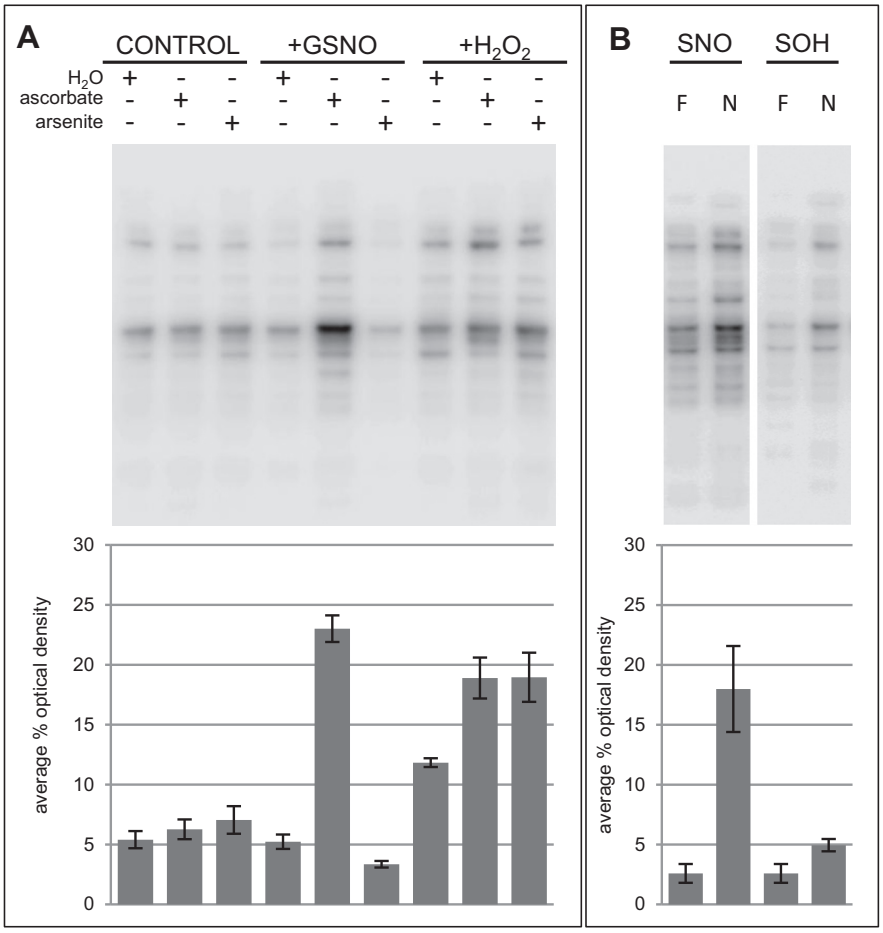

Fig. 2 – Induction of SNO and SOH in *E. coli* proteins. A. *In vitro* by treatment with GSNO (200 μM) or H_2O_2 (100 μM); B. *in vivo* by anaerobic growth on nitrate and in-culture stimulation with H_2O_2 (100 μM); SNO and SOH were detected by western blot using anti-TMT™ antibody (upper panels), densitometry analysis (n = 3) (lower panels). F — fumarate, N — nitrate.

To confirm that cellular metabolism was switched to anaerobic respiration using fumarate or nitrate as the terminal electron acceptor we performed label-free quantitative mass spectrometry of control (fumarate growth) and stressed (nitrate growth) samples. In total we have quantified 1581 proteins. From these, 669 proteins were significantly ($p \leq 0.05$) regulated between nitrate and fumarate grown bacteria (Table S2). The majority of the components of the dissimilatory nitrate reduction pathway were significantly increased in abundance in nitrate grown cells and fumarate reductase was increased in abundance in fumarate culture (Fig. 4). These data confirm that an anaerobic atmosphere was generated and resulted in a metabolic shift to fumarate or nitrate reduction, depending on the culture conditions.

Label-free quantitative proteomics results were compared to the results obtained from total cysteine labelling, where the samples were treated with TCEP, to reduce reversibly modified cysteines, and labelled with iodoTMT™ tags. The aim was to confirm that changes in protein levels measured by quantitation of cysteine-containing peptides will reflect the endogenous changes in protein abundance levels measured using the label-free approach. Comparison of the data obtained by the two approaches in 3 biological replicates showed a high correlation of $R^2 = 0.752 \pm 0.08$ (Fig. 5) supporting the applicability of total cysteine labelling for correction of protein abundance changes. Additionally these results further demonstrate that both iodoalkylation chemistry and iodoTMT™-based relative quantitation is robust in a simple system (total cysteines). Thus, we consider this chemistry to be applicable to the study of reversible cysteine modifications *e.g.* SOH.

In order to obtain estimates of global SNO/SOH levels in the analysed samples we have performed western blot analysis. This analysis provided an indication for the direction of SNO/SOH changes. The results show a clear increase in protein SNO induced by growth on nitrate as compared to fumarate (Fig. 2B and S3A). SOH although less pronounced was also induced. As anticipated, the total SNO and SOH levels were much lower than those obtained by *in vitro* oxidation induced by GSNO and H_2O_2 (Fig. 2A). These data are in line with the previously published work [6].

3.3. *Redox proteome of E. coli grown anaerobically on nitrate or fumarate*

The described SNO/SOH TMT strategy was applied to the *E. coli* model of mild oxidative stress. All unique, SNO/SOH

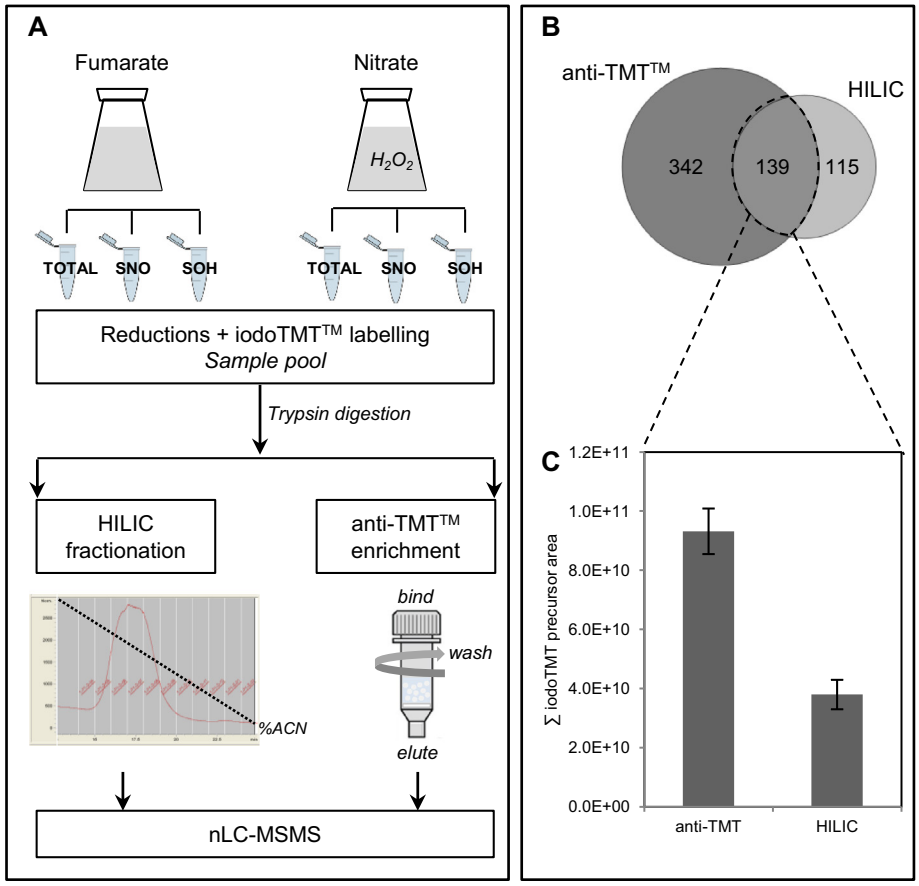

Fig. 3 – Reduced abundance of iodoTMT™-containing peptides when pre-fractionation replaces anti-TMT™ enrichment. A. Experimental design used to verify whether pre-fractionation can replace anti-TMT™ enrichment when dealing with low amount of starting material. B. Number of iodoTMT™ containing peptides identified using anti-TMT™ enrichment and HILIC fractionation (n = 3). C. Precursor area based quantitation was used to determine the difference in abundance between peptides identified by anti-TMT™ enrichment and HILIC.

containing peptides identified in all 3 biological replicates are listed together with their features in Table S3. In total we identified 480 unique peptides and 540 cysteine sites containing SNO, SOH or both modifications (Fig. 6A). Almost 66% of modified proteins were found with single cysteine SNO and/or SOH site (Fig. 6B). There were also 108 proteins containing multiple modification sites. Glutamate synthase [NADPH] large chain (P09831, GltB) was found with 8 oxidised cysteines. We have compared the identified proteins/sites to RedoxDB, currently the largest repository of experimental evidence for cysteine oxidative modifications [46]. From the 83 oxidatively modified proteins identified in this study only 16 are reported in RedoxDB. These 16 proteins cover 19 cysteine oxidation sites from which 7 match the site localisation from RedoxDB. Interestingly, for 4 of the matched sites, the modification type was not previously determined (Table S3).

In this work, quantitative results measuring levels of SNO and SOH modifications were only considered if the same peptide was found in the 3 biological replicates analysed (114 unique peptides). For 105 of those peptides (111 sites) SNO and SOH levels were quantified simultaneously. Additionally 8 peptides (from 8 proteins) contained only SNO. There were no peptides which exclusively contained iodoTMT™ reporter ions representing SOH modification. The 113 peptides containing both SNO/SOH and SNO only correspond to 90 proteins. The majority of these proteins are localised to the cytoplasm (37) several to membrane (8) and periplasm (3), many (42) were of unknown localization according to ontological information present in the Uniprot database (Fig. 6C). Network analysis using STRING (version 9.1) shows that the modified proteins cover several basic molecular pathways present in *E. coli* such as the Krebs cycle ($p = 3.2 \times 10^{-2}$, $n = 6$); alanine, aspartate and glutamate metabolism ($p = 1.1 \times 10^{-2}$, $n = 7$) and nitrogen metabolism ($p = 2.4 \times 10^{-2}$, $n = 7$) (Fig. 7).

3.3.1. *Changes in SNO and SOH levels between low and mild oxidative stress*

In order to evaluate the significance of the observed quantitative differences between low and mild oxidative stress we have used a 2 sigma approach. Results were log(2) transformed and normalised to the median. Normalised ratios for SNO and SOH were corrected for changes in protein abundance according to the ratio observed for total cysteine measurement.

In order to identify proteins with significant changes in SNO or SOH modification we adopted a two tier selection

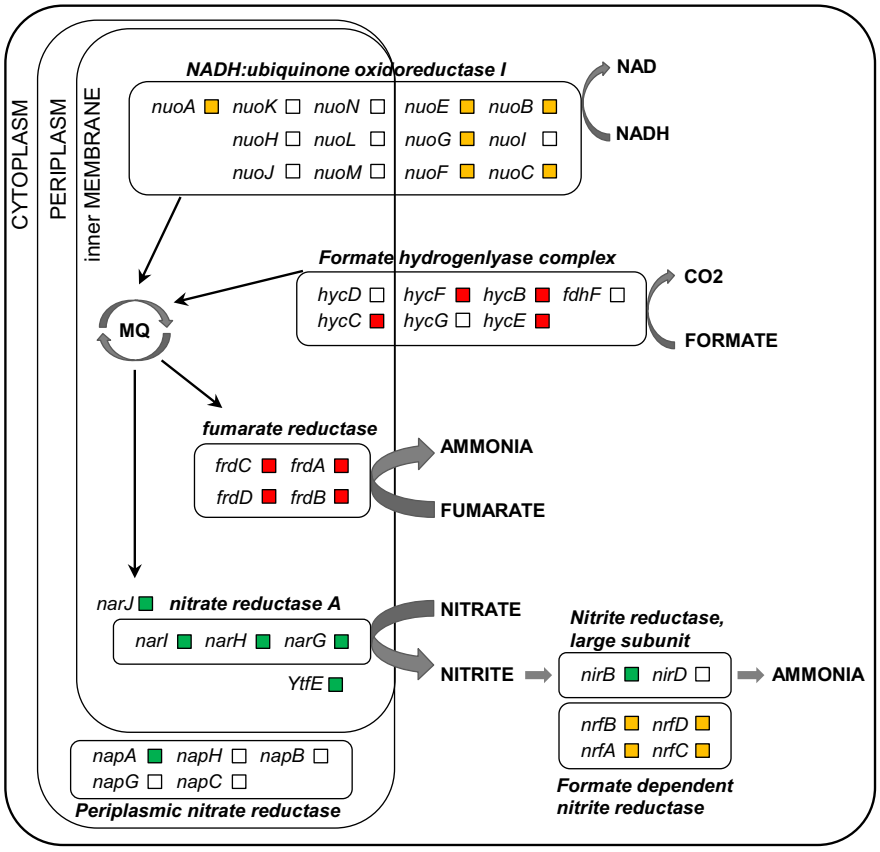

Fig. 4 – Respiratory pathways activated in *E. coli* grown anaerobically on nitrate as compared to fumarate. Label-free quantitative mass spectrometry was used to determine changes in protein abundance. The main protein complexes involved in anaerobic respiration are presented. Identified and quantified proteins are marked with coloured boxes. Colour code for fold changes in nitrate: green — increased, min. 2 fold, $p \leq 0.05$; red — decreased, min. 2 fold, $p \leq 0.05$; orange — no change, white (empty) — not identified.

criteria. The stringent criteria required that modified peptides were above 2 sigma fold change in SNO or SOH level in all 3 biological replicates. The relaxed criteria required 2 sigma fold change in 2 replicates.

Interestingly more than 80% of the quantified peptides showed no significant change in modification levels between the two experimental conditions. This may result from a moderate quantitation precision obtained in these experiments (Fig. S6). The quantitation precision for total cysteines was very high (average $R^2 = 0.769 \pm 0.01$), for SNO peptides was slightly lower (average $R^2 = 0.529 \pm 0.02$) and the largest inter-replicate variance was observed for SOH (average $R^2 = 0.200, \pm 0.06$). As discussed above, the quantitative precision is related to the reporter ion intensity which is linked to the abundance of the modifications in the sample. These data indicate that labelling more protein for SOH analysis would improve quantitative precision.

Despite this limitation, applying strict selection criteria, 6 of 105 peptides were found in altered abundance between fumarate and nitrate growth. These peptides belong to 3 proteins. Respiratory nitrate reductase 1 beta chain (P11349, NarH), fumarate reductase flavoprotein subunit (P00363, FrdA) and aldehyde–alcohol dehydrogenase (P0A9Q7, AdhE). Applying relaxed selection criteria revealed 10 more peptides which were quantified in at least 2 of the biological replicates. Among these, 2 were from fumarate reductase flavoprotein subunit and aldehyde–alcohol dehydrogenase with one additional peptide for each protein respectively. The remaining 8 peptides were from 8 distinct proteins. Table 2 lists the most differentially oxidised proteins together with modification fold change and relative site occupancy data. Fig. S7 provides annotated MSMS spectra of the modified peptides.

3.4. *Relative modification site occupancy*

A unique feature of SNO/SOH TMT approach is the ability of simultaneous quantification of peptides containing 3 cysteine forms: fully reduced, SNO and SOH modified. This allows us to calculate relative modification site occupancy. It is calculated as a percentage of reporter ion intensities from SNO and SOH cysteines, compared to total cysteines. It is important to stress that due to undetermined efficiency of ascorbate and arsenite reduction these site occupancy levels should only be considered as relative and not absolute values, therefore we refer to them as relative modification site occupancy. Results of SNO/SOH occupancy analysis are presented in Table 2 and Supplementary Table S3.

From this analysis we calculated the average site occupancy for each modification. These numbers should reflect the global levels of SNO or SOH in the analysed samples. The

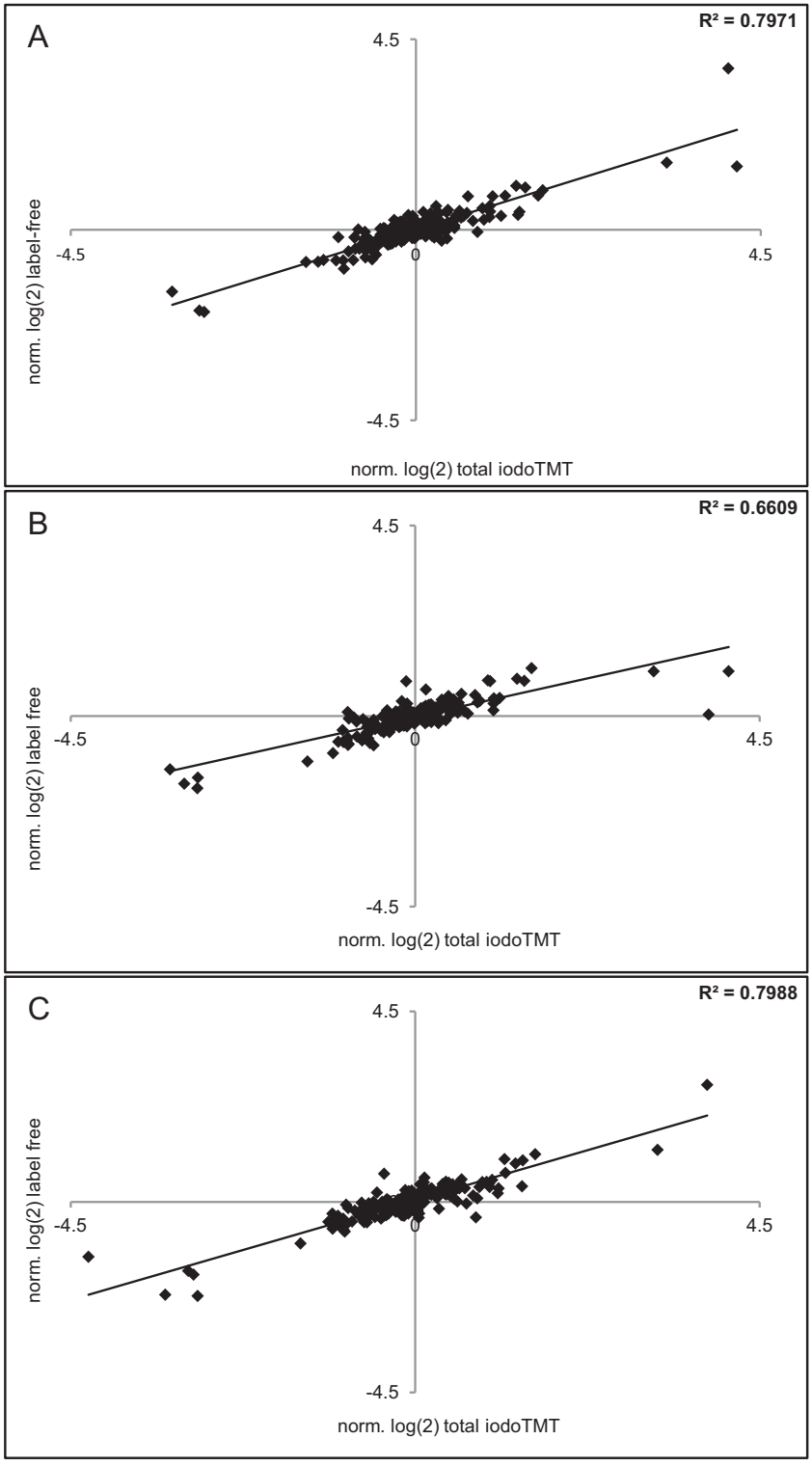

Fig. 5 – Correlation of protein abundance changes between label-free and total cysteines iodoTMT™ labelling approaches. Correlation coefficient (R^2) was calculated for each pair of respective replicates. Accordingly, A–C corresponds to replicates 1–3.

baseline level of SNO occupancy in fumarate growth was 3% increasing to 4.5% under nitrate growth. SOH exhibited approximately 1.1% occupancy under fumarate growth, increasing to 1.3% in stress conditions.

The relative occupancy of individual sites was also investigated. The residue with the largest percentage of SNO occupancy in nitrate grown *E. coli* was C184 of NarH with 21.2% ± 4.6 of residue modified. Interestingly this residue also

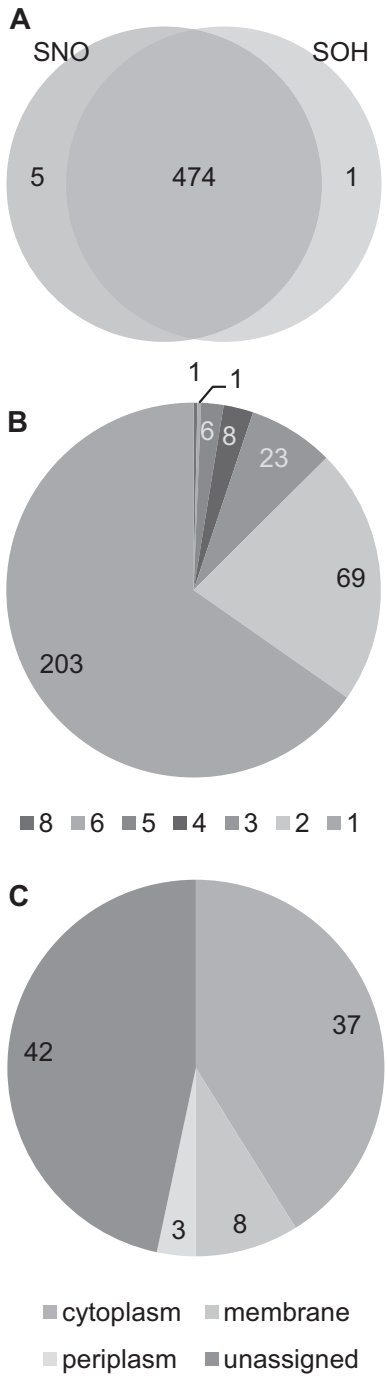

Fig. 6 – Distribution of SNO and SOH modifications in *E. coli* proteome under mild oxidative stress (n = 3). A. Overlap between SNO and SOH sites; B. number of SNO and SOH residues per protein; C. cellular localisation of SNO and SOH proteins.

exhibits the largest SOH occupancy 7.8% ± 4.3 (Fig. 8A). Respiratory nitrate reductase was also found to be among the most differentially oxidised proteins (see Table 2). The protein with the second highest relative site occupancy observed was NADP-specific glutamate dehydrogenase (P00370, GdhA). Its residue C147 was 12% ± 1.3 S-nitrosylated under nitrate growth (Fig. 8B). Interestingly neither the abundance of this protein nor its modification changed under mild oxidative stress. The third protein with largest SNO site occupancy was PTS-dependent dihydroxyacetone kinase, phosphotransferase subunit DhaM (P37349, DhaM). Here 10.5% ± 0.7 of C195 was modified under nitrate growth (Fig. 8C).

The second largest relative site occupancy by SOH was Protein YeeZ (P0AD12, YeeZ). Its residue C213 was 3.2% ± 0.7 S-sulfenylated in nitrate (Fig. 8D). Cysteine C45 of Ketol-acid reductoisomerase (P05793, IlvC) was the third most S-sulfenylated residue. Although the actual site occupancy was rather low 2.9% ± 0.4 (Fig. 8E). The examples of NarH and GdhA show that high occupancy does not necessarily imply that a particular site is differentially modified under stress. The fact that both relative abundance and relative site occupancy can be derived from a single experiment is therefore a considerable advantage of the SNO/SOH TMT method.

4. Discussion

4.1. SNO/SOH TMT strategy

Differential alkylation is a common strategy in studies of cysteine oxidation [2]. It is also the basis of the current work. Here we use iodoTMT™ providing a permanent mass tag that can be enriched and detected by mass spectrometry. Although isobaric iodoTMT™ tags allow for sample multiplexing [32] our strategy favours multifunctionality. We use isobaric iodoTMT™ tags for simultaneous analysis of 3 distinctive cysteine subsets in 2 experimental conditions. Our targets are total (TCEP reduced), S-nitrosylated and S-sulfenylated cysteines. The notable features of this approach are: 1) direct identification of modified cysteine; 2) correction of changes in protein modification levels by changes in protein abundance in a single experiment; 3) estimation of relative modification site occupancy; 4) simultaneous analysis of two different types of cysteine modification.

4.1.1. Identification of modified cysteines

In common with some other methods, our SNO/SOH TMT approach provides resolution of the site of modification [15,16,32]. This is of critical importance as it allows one to demonstrate if modifications are occurring in functionally important regions of a protein. For example, we identified several sites which coordinate iron–sulfur clusters and one example (AdhE) of an active site cysteine (discussed in more detail below).

4.1.2. Correction of changes in protein modification level by changes in protein abundance level in a single experiment

We have used the multiplexing capability of the iodoTMT™ labels to include a control where all TCEP reducible cysteines are derivatised. This allows correction of changes in protein modification levels by changes in protein abundance levels in a single experiment. Such correction is mandatory to depict true modification levels and rule out all alterations caused solely by changes in protein abundance levels, especially for studies where long-term treatment is applied. Such correction

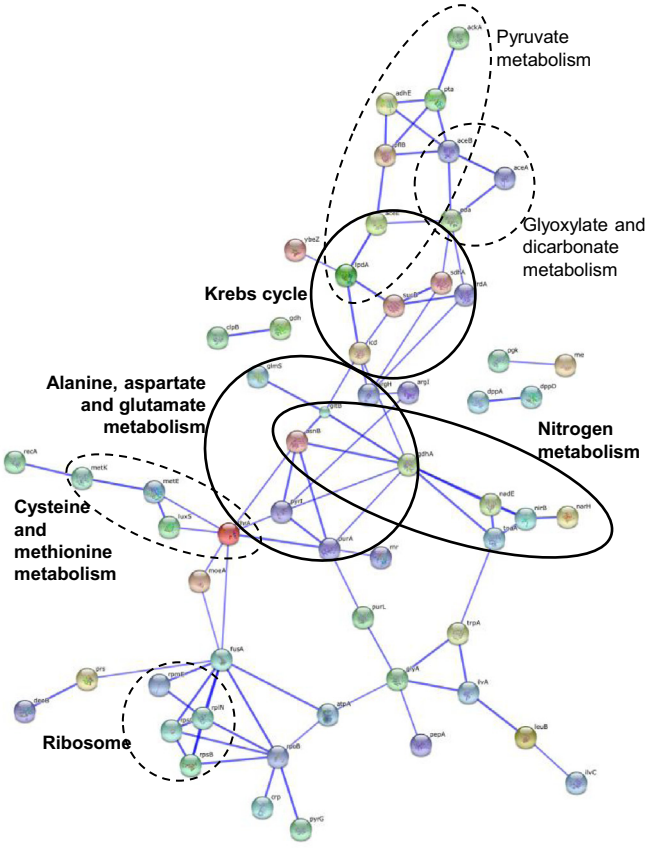

Fig. 7 – Interaction network of *E. coli* proteins modified (SNO/SOH) under mild oxidative stress. Continuous ovals — protein groups significantly enriched in the dataset; Dashed ovals — other, functionally associated proteins. Network analysis was performed using String version 9.1 with confidence view and confidence score of 0.700, no text mining was used.

has however rarely been implemented into previous thiol redox strategies, as reviewed in [2]. Most of the strategies attempting correction of modification levels by protein abundance changes rely on non-isobaric isotopic labelling which suffers from reduced sensitivity and multiplexing capability [23–25]. Furthermore, most of these protocols are laborious, requiring additional experiments employing alternative quantitation strategies and extensive fractionation to determine protein abundance changes [23,25]. We overcome these limitations in SNO/SOH TMT by using isobaric labels for relative quantitation. Despite the known issues with dynamic range compression due to precursor co-isolation in quantitation with isobaric tags [47], we achieved an excellent correlation of approx. 75% with label-free data. The slight discrepancies between the label-free and iodoTMT™ total cysteine labelling may originate from the contribution of other reversible and irreversible cysteine oxoforms, sulfinic and sulfonic acid. We recommend correcting SNO/SOH levels by protein abundance changes determined by total cysteine labelling as that should provide more accurate quantitation then when using label-free data for correction, which do not suffer from dynamic range compression.

4.1.3. Estimation of relative site occupancy

The quantitative information obtained from total cysteines can also be used to estimate the fraction of the residue occupied by the identified modification — relative modification site occupancy. This information is believed to have higher biological impact than the relative abundance [28]. For instance modification site occupancy determines level of enzyme inhibition and levels of protection against irreversible oxidations [4]. It is especially important when multiple PTMs are expected to occur at certain residue [26] allowing the investigation of interplay between modifications. There have been previous studies attempting to determine SNO site occupancy, one based on isobaric cysteine-reactive TMT™ tags [28], the other based on phenylmercury enrichment [27]. However, in these studies the contribution of oxidative cysteine modifications (S–S, S–GS, SOH) was either neglected [27] or required additional experimental steps to be implemented [28]. In our strategy, not only SNO but also, for the first time SOH site occupancy is measured as a percentage of total cysteines, all retrieved from single nLC-MSMS experiment. It should be noted that our SNO/SOH site occupancy relies on MMTS blocking efficiency and ascorbate/arsenite reduction specificity, which we did not fully assess. However, these crucial steps have been thoroughly evaluated by the others [6,48,49].

4.1.4. The ability to simultaneously analyse two different types of cysteine modifications

Methodologies, such as the one recently published by Guo et al. are powerful tools for studying cysteine redox proteomes [49]. They allow for parallelized analysis of virtually any

Table 2 – Proteins with the largest changes in SNO and/or SOH levels between nitrate (stressed) and fumarate (control) grown *E. coli*.

Protein name	UniProt acc.	Peptide sequence	Modified site(s)	Modification fold change log(2) between fumarate and nitrate growth [a, b]						Relative site occupancy (%) [c]			
				SNO			SOH			SNO F	SNO N	SOH F	SOH N
Aldehyde–alcohol dehydrogenase	P0A9Q7	TFDNGVIcASEQSVVVVDSVYDAVR	C246	**1.798**	**1.719**	**1.164**	**1.373**	**1.301**	0.408	1.6	6.8	0.8	1.6
		LVAmGGIGHTScLYTDQDNQPAR	C370	**1.656**	**1.992**	**1.646**	0.372	**1.256**	−0.346	0.8	4.0	0.8	1.2
		LAPSLTLGcGSWGGNSISENVGPK	C421	**1.252**	**1.197**	**1.905**	**1.319**	0.765	0.137	1.4	5.0	0.5	1.0
		LSEDAFDDQcTGANPR	C841	**1.704**	**1.250**	n/a	1.172	0.586	n/a	1.5	6.1	0.9	1.7
Fumarate reductase flavoprotein subunit	P00363	GLFAVGEcSSVGLHGANR	C381	**1.497**	**1.508**	**1.612**	1.091	**1.561**	1.189	1.8	7.6	0.7	1.9
		IRDEmGLAmEEGcGIYR	C464	**1.280**	**1.174**	**1.682**	0.447	0.540	0.202	1.4	5.4	1.0	1.7
		EPIPVRPTAHYTmGGIETDQNcETR	C368	**1.868**	**1.654**	n/a	1.206	**1.959**	n/a	0.9	4.3	0.5	1.7
Respiratory nitrate reductase 1 beta chain	P11349	LcEHcLNPAcVATcPSGAIYK	C184	0.146	0.217	−0.003	**1.734**	**1.209**	**1.093**	13.3	21.2	2.4	7.8
Acetolactate synthase isozyme 1 large subunit	P08142	TDGKPAVcmAcSGPGATNLVTAIADAR	C80, C83	**−1.235**	0.018	**−2.299**	−1.196	0.631	**−2.667**	3.4	1.5	0.5	0.2
Acetolactate synthase isozyme 1 small subunit	P0ADF8	NHPGVmTHVcGLFAR	C26	n/a	**−1.065**	**−1.353**	n/a	−0.935	−1.205	5.2	3.6	1.7	0.9
Fumarate reductase iron–sulfur subunit	P0AC47	mAIcGScGmmVNNVPK	C63, C66	n/a	**1.007**	**1.978**	n/a	**2.090**	n/a	0.6	2.5	0.5	1.9
Nitrite reductase [NAD(P)H] large subunit	P08201	SDAANFDITVFcEEPR	C37	−0.890	**−1.206**	**−0.992**	−0.579	−1.027	−0.057	3.2	2.3	0.9	0.7
Peptidase T	P29745	DcDIEPELKPIR	C343	n/a	0.743	0.540	n/a	**1.285**	**1.618**	6.1	15.5	1.7	4.2
Probable dimethyl sulfoxide reductase chain YnfF	P77783	cPEEHYVAFR	C614	**1.529**	**1.044**	n/a	**1.583**	**1.773**	n/a	2.5	8.9	1.1	3.6
UPF0263 protein YciU	P0A8L7	LcHIIWR	C103	0.538	n/a	−0.001	**2.143**	n/a	**1.335**	2.7	4.6	0.3	1.2
Bifunctional aspartokinase/homoserine dehydrogenase 1	P00561	YVGNIDEDGVcR	C755	0.701	**1.481**	n/a	**1.726**	0.757	n/a	0.4	1.0	0.1	0.2

n/a — not available.

[a] log(2) normalised and corrected by protein abundance change values.

[b] Significant modification change (≥2 sigma) are marked in bold; individual 2 sigma values were as follows SNO: 0.940, 0.956, and 0.991, SOH: 1.308, 1.054, and 1.081 for each replica respectively;

[c] % SNO/SOH site occupancy was calculated based on raw reporter ion intensities in relation to total cysteines from fumarate (F) or nitrate (N) grown *E. coli*.

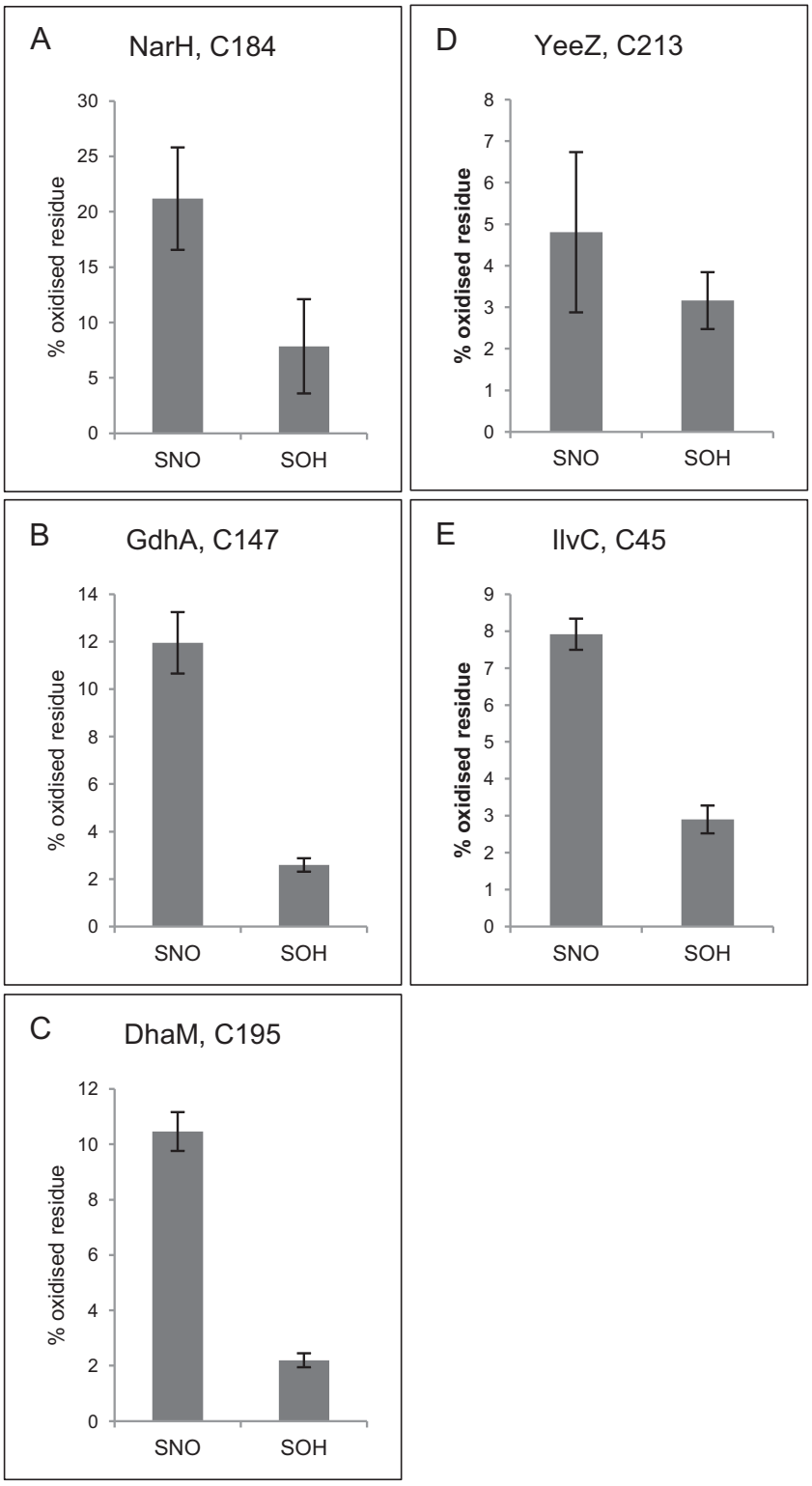

Fig. 8 – Modification site occupancy under nitrate growth. Peptides with the highest site occupancy for SNO (A–C) and SOH (A, D–E) are presented.

reversible cysteine modification. However, the unique design of SNO/SOH TMT approach provides, for the first time, simultaneous detection and quantitation of two distinct, reversible cysteine modifications, SNO and SOH. As discussed below, this allows us to shed light on the relationship between these two modifications and for the first time investigate possible cross-talk between these modifications.

4.2. Optimisation of SNO/SOH TMT strategy

The fundamentals of SNO/SOH TMT strategy are based on iodoTMT™ protocols provided by the manufacturers (Thermo Scientific). However new elements have been added and optimisation was performed to accommodate the novel features of the method. The most critical optimisation work is discussed below.

4.2.1. MMTS blocking of reduced sulfhydryl groups

Efficient blocking of free sulfhydryl groups (–SH) present in protein extracts is a mandatory step to ensure no artifactual increase in the observed cysteine oxidation levels. It can be achieved by using MMTS [50,51], N-ethylmaleimide (NEM) [24,52] or IAA [25] each with unique advantages and limitations as reviewed in [53]. We have chosen to use MMTS because the reaction pH is compatible with downstream sample processing, which increases throughput of sample preparation and minimises sample losses. Additionally, unlike NEM, MMTS labelling is reversible and can be replaced with IAA prior to trypsin digestion. This minimises the number of modifications that must be used for subsequent searches of MS-derived data, reducing database search space and false discovery rate. In our hands, the efficiency of free thiol blocking was maximised when the blocking reaction was performed directly during cell lysis. For *E. coli* a MMTS concentration of 50 mM at a ratio of 33 nmol per 1 μg of protein yielded, although not complete, however, relatively effective blocking. The SNO/SOH TMT approach can be easily combined with any blocking/alkylation reagent, *e.g.* MMTS, NEM or IAA. We highly recommend evaluation of efficiency for each type of blocking/alkylation reagent and biological sample by *e.g.* western blot analysis. Additionally, complete removal of unbound blocking reagent prior to reduction and alkylation is required. Otherwise it may compete with iodoTMT™ hampering the detection of target sulfhydryl groups [50].

4.2.2. Differential alkylation of SNO, SOH and total cysteines

Differential alkylation is a balance between selectivity of modification specific reductants and efficiency and stability of alkylating chemistry. Despite widespread usage, the selectivity of SNO reduction by ascorbate and SOH reduction by arsenite has been controversial as reviewed in [2]. This is due to the apparent concentration dependent changes in reactivity of the reducing agents [48,54,55]. However, many publications also demonstrate that non-selective reduction is in the minority and often results from sample preparation artefacts rather than from erroneous chemistry [48,56]. We have observed GSNO and H_2O_2 induced formation of SNO and SOH and tested the selectivity of ascorbate and arsenite reduction and iodoTMT™ alkylation. Increased signal intensity in oxidised samples under modification specific reduction conditions as compared to the control confirm that the reaction conditions used favoured the selectivity of SNO and SOH reduction respectively. Although we believe that our method is reliable in profiling alterations in cysteine modifications, it is only as reliable as the chemistry on which it is based therefore we emphasise the need for further validation with complementary methods like *e.g.* UV photolysis [57] or anti-S-nitrosocysteine antibody for SNO and dimedone labelling for SOH [19,20].

In case of total cysteine labelling, we observed that in addition to the use of an appropriate reagent concentration the sequence of reduction/alkylation steps is also important. Sequential reduction, reducing agent removal and alkylation is essential for complete TCEP reduction. In the case of modification specific reductions, reduction and alkylation may be performed simultaneously [40]. Quenching and removal of excess of the derivatization reagent are mandatory prior to subsequent detection by selective affinity enrichment as well as by western blot [40,58]. Partially neutralised tags might cross-react with cysteines where MMTS is released during reduction, artifactually increasing overall signal intensity. We have observed this by western blot, and found that 500 mM DTT for quenching was sufficient to ameliorate this effect (Supplementary Fig. S3B). 500 mM DTT provides excess of free SH groups sufficient to neutralise unbound iodoTMT™ tags used for both SNO/SOH labelling (10 000 times excess of SH groups over initial iodoTMT™ concentration used for labelling) and for total cysteine labelling (200 times excess). This is much higher than what is typically used in similar studies [23].

4.2.3. Anti-TMT™ enrichment and alternative purification strategies

Optimised enrichment schemes are powerful tools in modification specific proteomics [59]. Therefore selective enrichment of iodoTMT™ labelled peptides is an important element of the presented strategy. We have achieved 7% enrichment of iodoTMT™ containing peptides with the anti-TMT™ antibody which is in line with other antibody based pull-downs of PTMs. For example, anti-(lysine) acetyl antibody typically recovers 10–20% acetylated peptides [60]. Based on our results it is clear that the overall enrichment strategy is severely affected by the abundance of labelled peptides. We sought to investigate whether orthogonal pre-fractionation (in this case by HILIC chromatography) followed by extensive MS analysis would compensate for lack of iodoTMT™-specific enrichment. We used 100 times less material (20 μg) for HILIC pre-fractionation compared to what was enriched with anti-TMT™ resin. This amount of starting material could be compatible with analysis of difficult to obtain biological samples such as human tissue biopsies. Additionally, the hands-on time for the HILIC method is much less than the anti-TMT™ enrichment approaches. Even with 100 times less material, a large number of iodoTMT™-containing peptides were identified with relatively large proportion of uniquely identified peptides. Poor overlap between anti-TMT™ enrichment and HILIC pre-fractionation might be purely due to stochastic nature of data-dependent acquisition and limited number of technical replicates. Alternatively, it might be due to orthogonal character of the two techniques. In any case, the quantitative precision in the HILIC pre-fractionated samples was severely compromised due to lower (1 order of magnitude) reporter ion intensity. In the future improvements should be sought aiming at increasing the number of identified SNO/SOH modified peptides with focus on maintaining high quality of the quantitative information without demanding high sample quantities.

4.2.4. Reproducibility and analytical precision

This is the first study aiming at global, quantitative profiling of SNO and SOH changes in *E. coli* under mild oxidative stress. In total we have identified 540 SNO/SOH sites. We achieved good quantitative precision for both total cysteine labelling and SNO across 3 biological replicates. However, analysis of SOH sites was more challenging. Although we identified a reasonable number of SOH sites, quantitative information was somewhat compromised. One possible explanation is that near physiological levels of oxidative stress imposed on our model did not induce extensive SOH. This is also suggested by western blot analysis. Alternatively, SOH might have undergone further transformation to either reversible (SNO, disulfide bonds) or irreversible modifications (S-sulfination, S-sulfonation) prior to selective reduction and irreversible blocking with iodoTMT™.

4.3. Co-occurrence of SNO and SOH

Our data clearly show that in the vast majority of cases SNO and SOH may occupy the same site, allowing for interaction and cooperation between the modifications. This is in agreement with the study of Kohr and co-workers who established the relevance of interplay between SNO and other cysteine modifications in the context of ischemia reperfusion injury [29]. This is contrary to a previous work which suggested that these modifications are almost exclusive [22]. However, in this study modifications were identified in parallel whereas we believe that in order to precisely detect interplay between SNO and SOH a technique for simultaneous detection of these modifications (such as SNO/SOH TMT) must be used. Our method may be further adapted to address other unanswered questions. To give a specific example, the interplay between disulfide bond formation, glutathionylation and SNO of Cys294, a known redox switch of the Mammalian ATP synthase, has not been measured simultaneously in quantitative manner [61].

4.4. Relative site occupancy

We observed that, with the notable exception of C184 from respiratory nitrate reductase 1 beta chain, sites with high SNO and SOH occupancy were not differentially regulated between the two conditions. For instance, cysteine 147 of NADP-specific glutamate dehydrogenase was the second most heavily S-nitrosylated site, even though neither the protein abundance nor the level of SNO was found differentially regulated. This demonstrates that the presence or absence of a modification is not necessarily indicative of its biological role in a given system. These data support the idea that the extent of cysteine modification may have a bearing on the role of that modification [62]. For instance, a low abundance modification may play a role in signalling, moderate abundance may function as an antioxidant buffer and high abundance may indicate oxidative damage.

4.5. SNO/SOH TMT strategy detects endogenous SNO and SOH levels

Until today a large number of studies use experimental models in which the oxidation is chemically induced with *e.g.* GSNO [30,31]. In those models the oxidation level is typically very high and often performed in denaturing conditions where alterations in protein structure can readily affect the potential of cysteine to undergo modification. Therefore in this study we aimed to induce a mild level of oxidative stress in *E. coli* to test if the SNO/SOH TMT method was applicable where physiological levels of oxidative modifications are present. Protein expression analysis has confirmed that *E. coli* has switched its metabolism to anaerobic growth in nitrate or fumarate. Our data are largely in agreement with a microarray study of a similar model system [6]. Of the genes up-regulated under nitrate growth and their corresponding proteins in the present study, 68% agree in the direction of regulation (Table S2). From these data we can also observe only three proteins moderately increased in abundance (Thiol peroxidase, Superoxide dismutase [Cu–Zn], Alkyl hydroperoxide reductase subunit C) from the *E. coli* antioxidant machinery, indicating that the oxidative insult was indeed relatively mild.

In relation to oxidative modifications, our findings reflect those of Murray et al. [63]. The relative abundance of the majority of modified cysteines did not change between low (fumarate growth) and mild (nitrate growth) oxidative stress. The proteins with the most differential modification in our study were NarH (C184-SOH); FrdA (Cys381 + 464-SNO) and AdhE (Cys246, 370, 421-SNO). These, along with YncF, PepT and FrdB all coordinate iron–sulfur clusters, use metal ions as cofactors or are present in a complex which contains iron–sulfur proteins. This is to be expected as proximity to metal ions is a risk factor for oxidation. In concert with the multiple observations of oxidatively modified metal coordinating proteins, we observe a significant increase in abundance of iron–sulfur cluster repair proteins YtfE, SufB and SufC in the label-free data. This is a further indication that metal ion proximal proteins are particularly susceptible to modification, even under mild oxidative conditions.

Modification of NarH is localised to C184, which is one of the cysteines coordinating one of the three iron–sulfur clusters bound by NarH (Fig. 9). This modification could affect the function of the protein as has been described for the master regulator of the switch to anaerobic growth FNR [64]. Interestingly, although this site has one of the highest relative site occupancy for both SNO and SOH, a significant change between low and mild oxidative stress has been observed only for SOH. It is likely that the high levels of SNO result from its proximity to NarG which is the major source of SNO in *E. coli* [6]. The high basal level of SNO could be the reason why no significant increase in mild stress conditions is observed. The modification to C246 of AdhE is particularly interesting as this residue forms part of the enzyme active site and its modification will certainly result in loss of enzyme activity. These findings are in line with published data regarding the susceptibility of aldehyde–alcohol dehydrogenase to oxidative modifications, particularly to metal-catalysed oxidation [65,66].

The SNO/SOH TMT technique presented was able to produce quantitative, biologically relevant data relating to SNO and SOH in a system under relatively mild oxidative stress. These data also highlight the need for quantitative information in such studies since high site occupancy does

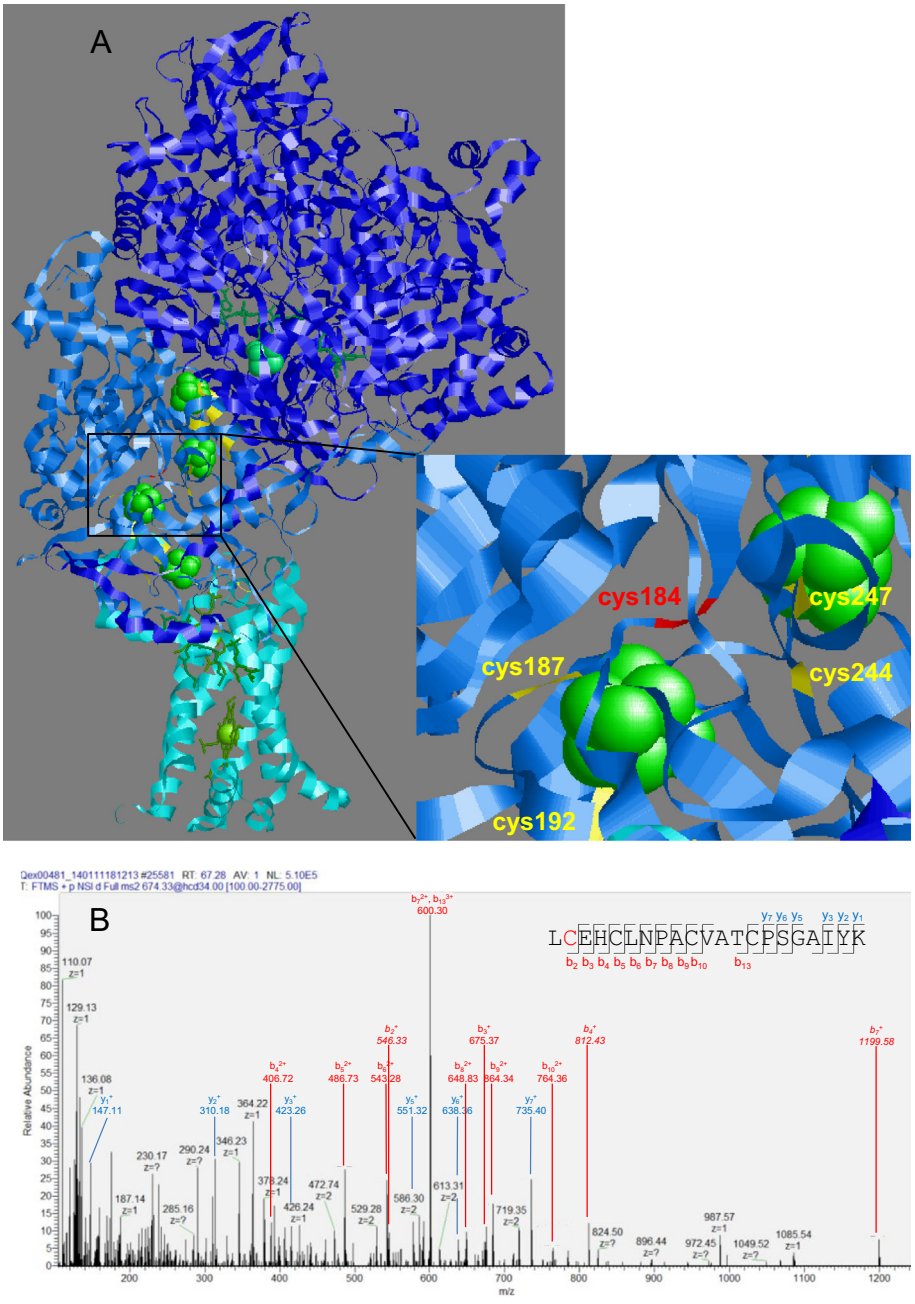

Fig. 9 – SNO and SOH modifications of cysteine 184 residue in nitrate reductase A (NarH) of *Escherichia coli*. A. Structural model of NarH complex, (PDB 1Q16). Dark blue — NarG; light blue — NarH; cyan — NarI; green — iron–sulfur cluster and other cofactors; yellow — cysteine residues of NarH. Insert — enlarged fragment of NarH structure with the differentially modified cysteine residue Cys 184. B. MSMS fragmentation of peptide LCEHCLNPACVATCPSGAIYK, with fragment ions resolving position of the modification site.

not necessarily equate to a site of modification which responds to oxidative stress.

5. Conclusions

We present a new strategy for the analysis of protein SNO and SOH modifications, identification, quantitation, modification site localisation, correction of cysteine oxidation levels by protein abundance changes and determination of relative modification site occupancy in a single nLC-MSMS experiment. Importantly, SNO/SOH TMT strategy allows for simultaneous analysis of SNO and SOH changes in samples with physiological levels of oxidative stress. All based on commercially available Iodoacetyl Tandem Mass Tag reagents (iodoTMT™, Thermo Scientific).

SNO/SOH TMT is a powerful methodology for simultaneous screening of SNO and SOH alterations in response to

changes in ROS/RNS levels providing candidates for further functional validation with alternative strategies.

This method creates completely new possibilities to study the interdependence between SNO and SOH in biological systems. It is anticipated that this approach, applied for the analysis of biological questions will contribute to our understanding of how cellular redox is sensed and transduced to a functional effect by protein thiol redox sensors. This will help us better appreciate the role of oxidants in health and disease.

Supplementary data to this article can be found online at http://dx.doi.org/10.1016/j.jprot.2014.10.015.

Transparency document

The Transparency document associated with this article can be found, in the online version.

Acknowledgements

We would like to express our gratitude to Dr. Veit Schwämmle for help with significance analysis, Professor Peter Højrup and Kristina Egede Budtz for amino acid composition analysis. The authors were financially supported by — Sino-Danish Center For Education and Research (KW), Augustinus Fonden, Journ. nr. 13-3455 (KW), The Danish National Research Foundation's Centre for Epigenetics DNRF82 (JW), Department of Biochemistry and Molecular Biology, University of Southern Denmark (ARW).

REFERENCES

[1] Bachi A, Dalle-Donne I, Scaloni A. Redox proteomics: chemical principles, methodological approaches and biological/biomedical promises. Chem Rev 2013;113:596–698.
[2] Held JM, Gibson BW. Regulatory control or oxidative damage? Proteomic approaches to interrogate the role of cysteine oxidation status in biological processes. Mol Cell Proteomics 2012;11 R111.013037.
[3] Foster MW, Hess DT, Stamler JS. Protein S-nitrosylation in health and disease: a current perspective. Trends Mol Med 2009;15:391–404.
[4] Murphy E, Kohr M, Menazza S, Nguyen T, Evangelista A, Sun J, et al. Signaling by S-nitrosylation in the heart. J Mol Cell Cardiol 2014;73:18–25.
[5] Gupta V, Carroll KS. Sulfenic acid chemistry, detection and cellular lifetime. Biochim Biophys Acta 1840;2014:847–75.
[6] Seth D, Hausladen A, Wang YJ, Stamler JS. Endogenous protein S-Nitrosylation in *E coli*: regulation by OxyR. Science 2012;336:470–3.
[7] Kettenhofen NJ, Wood MJ. Formation, reactivity, and detection of protein sulfenic acids. Chem Res Toxicol 2010;23:1633–46.
[8] Leonard SE, Carroll KS. Chemical 'omics' approaches for understanding protein cysteine oxidation in biology. Curr Opin Chem Biol 2011;15:88–102.
[9] Claiborne A, Yeh JI, Mallett TC, Luba J, Crane III EJ, Charrier V, et al. Protein-sulfenic acids: diverse roles for an unlikely player in enzyme catalysis and redox regulation. Biochemistry 1999;38:15407–16.
[10] van Montfort RL, Congreve M, Tisi D, Carr R, Jhoti H. Oxidation state of the active-site cysteine in protein tyrosine phosphatase 1B. Nature 2003;423:773–7.
[11] Wood ZA, Poole LB, Karplus PA. Peroxiredoxin evolution and the regulation of hydrogen peroxide signaling. Science 2003;300:650–3.
[12] Antelmann H, Helmann JD. Thiol-based redox switches and gene regulation. Antioxid Redox Signal 2011;14:1049–63.
[13] Giron P, Dayon L, Sanchez JC. Cysteine tagging for MS-based proteomics. Mass Spectrom Rev 2011;30:366–95.
[14] Jaffrey SR, Snyder SH. The biotin switch method for the detection of S-nitrosylated proteins. Sci STKE 2001;2001:pl1.
[15] Leichert LI, Gehrke F, Gudiseva HV, Blackwell T, Ilbert M, Walker AK, et al. Quantifying changes in the thiol redox proteome upon oxidative stress in vivo. Proc Natl Acad Sci U S A 2008;105:8197–202.
[16] Sethuraman M, McComb ME, Huang H, Huang S, Heibeck T, Costello CE, et al. Isotope-coded affinity tag (ICAT) approach to redox proteomics: identification and quantitation of oxidant-sensitive cysteine thiols in complex protein mixtures. J Proteome Res 2004;3:1228–33.
[17] Qu Z, Meng F, Bomgarden RD, Viner RI, Li J, Rogers JC, et al. Proteomic quantification and site-mapping of S-nitrosylated proteins using isobaric iodoTMT reagents. J Proteome Res 2014;13:3200–11.
[18] Saurin AT, Neubert H, Brennan JP, Eaton P. Widespread sulfenic acid formation in tissues in response to hydrogen peroxide. Proc Natl Acad Sci U S A 2004;101:17982–7.
[19] Benitez LV, Allison WS. The inactivation of the acyl phosphatase activity catalyzed by the sulfenic acid form of glyceraldehyde 3-phosphate dehydrogenase by dimedone and olefins. J Biol Chem 1974;249:6234–43.
[20] Poole LB, Zeng BB, Knaggs SA, Yakubu M, King SB. Synthesis of chemical probes to map sulfenic acid modifications on proteins. Bioconjug Chem 2005;16:1624–8.
[21] Reddie KG, Seo YH, Muse Iii WB, Leonard SE, Carroll KS. A chemical approach for detecting sulfenic acid-modified proteins in living cells. Mol Biosyst 2008;4:521–31.
[22] Leonard SE, Reddie KG, Carroll KS. Mining the thiol proteome for sulfenic acid modifications reveals new targets for oxidation in cells. ACS Chem Biol 2009;4:783–99.
[23] Garcia-Santamarina S, Boronat S, Espadas G, Ayte J, Molina H, Hidalgo E. The oxidized thiol proteome in fission yeast—optimization of an ICAT-based method to identify H2O2-oxidized proteins. J Proteomics 2011;74:2476–86.
[24] Martinez-Acedo P, Nunez E, Gomez FJ, Moreno M, Ramos E, Izquierdo-Alvarez A, et al. A novel strategy for global analysis of the dynamic thiol redox proteome. Mol Cell Proteomics 2012;11:800–13.
[25] Garcia-Santamarina S, Boronat S, Domenech A, Ayte J, Molina H, Hidalgo E. Monitoring in vivo reversible cysteine oxidation in proteins using ICAT and mass spectrometry. Nat Protoc 2014;9:1131–45.
[26] Murray CI, Van Eyk JE. A twist on quantification: measuring the site occupancy of S-nitrosylation. Circ Res 2012;111:1253–5.
[27] Doulias PT, Tenopoulou M, Raju K, Spruce LA, Seeholzer SH, Ischiropoulos H. Site specific identification of endogenous S-nitrosocysteine proteomes. J Proteomics 2013;92:195–203.
[28] Kohr MJ, Aponte A, Sun J, Gucek M, Steenbergen C, Murphy E. Measurement of S-nitrosylation occupancy in the myocardium with cysteine-reactive tandem mass tags: short communication. Circ Res 2012;111:1308–12.
[29] Kohr MJ, Sun J, Aponte A, Wang G, Gucek M, Murphy E, et al. Simultaneous measurement of protein oxidation and S-nitrosylation during preconditioning and ischemia/reperfusion injury with resin-assisted capture. Circ Res 2011;108:418–26.
[30] Feng JH, Jing FB, Fang H, Gu LC, Xu WF. Expression, purification, and S-nitrosylation of recombinant histone deacetylase 8 in *Escherichia coli*. Biosci Trends 2011;5:17–22.

[31] Shi Q, Feng J, Qu H, Cheng YY. A proteomic study of S-nitrosylation in the rat cardiac proteins in vitro. Biol Pharm Bull 2008;31:1536–40.
[32] Pan KT, Chen YY, Pu TH, Chao YS, Yang CY, Bomgarden RD, et al. Mass spectrometry-based quantitative proteomics for dissecting multiplexed redox cysteine modifications in nitric oxide-protected cardiomyocyte under hypoxia. Antioxid Redox Signal 2014;20:1365–81.
[33] Neidhardt FC, Bloch PL, Smith DF. Culture medium for enterobacteria. J Bacteriol 1974;119:736–47.
[34] Gobom J, Nordhoff E, Mirgorodskaya E, Ekman R, Roepstorff P. Sample purification and preparation technique based on nano-scale reversed-phase columns for the sensitive analysis of complex peptide mixtures by matrix-assisted laser desorption/ionization mass spectrometry. J Mass Spectrom 1999;34:105–16.
[35] Wojdyla K, Rogowska-Wrzesinska A, Wrzesinski K, Roepstorff P. Mass spectrometry based approach for identification and characterisation of fluorescent proteins from marine organisms. J Proteomics 2011;75:44–55.
[36] The Global Proteome Machine. The common repository of adventitious proteins, cRAP. http://www.thegpm.org/cRAP/index.html.
[37] Leon IR, Schwammle V, Jensen ON, Sprenger RR. Quantitative assessment of in-solution digestion efficiency identifies optimal protocols for unbiased protein analysis. Mol Cell Proteomics 2013;12:2992–3005.
[38] Masuda T, Tomita M, Ishihama Y. Phase transfer surfactant-aided trypsin digestion for membrane proteome analysis. J Proteome Res 2008;7:731–40.
[39] Verano-Braga T, Miethling-Graff R, Wojdyla K, Rogowska-Wrzesinska A, Brewer JR, Erdmann H, et al. Insights into the cellular response triggered by silver nanoparticles using quantitative proteomics. ACS Nano 2014;8:2161–75.
[40] Thermo Scientific Instructions. Iodoacetyl tandem mass TagTM (iodoTMT™) reagents. http://www.piercenet.com/instructions/2162387.pdf.
[41] Kim SO, Merchant K, Nudelman R, Beyer Jr WF, Keng T, DeAngelo J, et al. OxyR: a molecular code for redox-related signaling. Cell 2002;109:383–96.
[42] Lin A, Wang Y, Tang J, Xue P, Li C, Liu L, et al. Nitric oxide and protein S-nitrosylation are integral to hydrogen peroxide-induced leaf cell death in rice. Plant Physiol 2012;158:451–64.
[43] Htet Hlaing K, Clement MV. Formation of protein S-nitrosylation by reactive oxygen species. Free Radic Res 2014;1–37.
[44] Dujovne CA. Liver cell culture toxicity and surfactant potency of erythromycin derivatives. Toxicol Appl Pharmacol 1975;32:11–20.
[45] Halliwell B, Gutteridge JMC. Free radicals in biology and medicine. 4th ed. Oxford. New York: Oxford University Press; 2007.
[46] Sun MA, Wang Y, Cheng H, Zhang Q, Ge W, Guo D. RedoxDB—a curated database for experimentally verified protein oxidative modification. Bioinformatics 2012;28:2551–2.
[47] Ow SY, Salim M, Noirel J, Evans C, Rehman I, Wright PC. iTRAQ underestimation in simple and complex mixtures: "the good, the bad and the ugly". J Proteome Res 2009;8:5347–55.
[48] Forrester MT, Foster MW, Benhar M, Stamler JS. Detection of protein S-nitrosylation with the biotin-switch technique. Free Radic Biol Med 2009;46:119–26.
[49] Guo J, Gaffrey MJ, Su D, Liu T, Camp II DG, Smith RD, et al. Resin-assisted enrichment of thiols as a general strategy for proteomic profiling of cysteine-based reversible modifications. Nat Protoc 2014;9:64–75.
[50] Jaffrey SR, Erdjument-Bromage H, Ferris CD, Tempst P, Snyder SH. Protein S-nitrosylation: a physiological signal for neuronal nitric oxide. Nat Cell Biol 2001;3:193–7.
[51] Smith DJ, Maggio ET, Kenyon GL. Simple alkanethiol groups for temporary blocking of sulfhydryl groups of enzymes. Biochemistry 1975;14:766–71.
[52] Partis MD. Cross-linking of protein by ω-maleimido alkanoyl N-hydroxysuccinimido esters. J Protein Chem 1983;2:263–77.
[53] Hansen RE, Winther JR. An introduction to methods for analyzing thiols and disulfides: reactions, reagents, and practical considerations. Anal Biochem 2009;394:147–58.
[54] Holmes AJ, Williams DLH. Reaction of ascorbic acid with S-nitrosothiols: clear evidence for two distinct reaction pathways. J Chem Soc Perkin Trans 2 2000:1639–44.
[55] Wang X, Kettenhofen NJ, Shiva S, Hogg N, Gladwin MT. Copper dependence of the biotin switch assay: modified assay for measuring cellular and blood nitrosated proteins. Free Radic Biol Med 2008;44:1362–72.
[56] Murray CI, Van Eyk JE. Chasing cysteine oxidative modifications: proteomic tools for characterizing cysteine redox status. Circ Cardiovasc Genet 2012;5:591.
[57] Stamler JS, Jaraki O, Osborne J, Simon DI, Keaney J, Vita J, et al. Nitric oxide circulates in mammalian plasma primarily as an S-nitroso adduct of serum albumin. Proc Natl Acad Sci U S A 1992;89:7674–7.
[58] Thermo Scientific Instructions. Pierce S-nitrosylation western blot kit. http://www.piercenet.com/product/s-nitrosylation-western-blot-kit.
[59] Mertins P, Qiao JW, Patel J, Udeshi ND, Clauser KR, Mani DR, et al. Integrated proteomic analysis of post-translational modifications by serial enrichment. Nat Methods 2013;10:634–7.
[60] Guan KL, Yu W, Lin Y, Xiong Y, Zhao S. Generation of acetyllysine antibodies and affinity enrichment of acetylated peptides. Nat Protoc 2010;5:1583–95.
[61] Wang SB, Foster DB, Rucker J, O'Rourke B, Kass DA, Van Eyk JE. Redox regulation of mitochondrial ATP synthase: implications for cardiac resynchronization therapy. Circ Res 2011;109:750–7.
[62] Thamsen M, Jakob U. The redoxome: proteomic analysis of cellular redox networks. Curr Opin Chem Biol 2011;15:113–9.
[63] Murray CI, Uhrigshardt H, O'Meally RN, Cole RN, Van Eyk JE. Identification and quantification of S-nitrosylation by cysteine reactive tandem mass tag switch assay. Mol Cell Proteomics 2012;11 M111 013441.
[64] Crack JC, Stapleton MR, Green J, Thomson AJ, Le Brun NE. Mechanism of [4Fe-4S](Cys)4 cluster nitrosylation is conserved among NO-responsive regulators. J Biol Chem 2013;288:11492–502.
[65] Moon KH, Abdelmegeed MA, Song BJ. Inactivation of cytosolic aldehyde dehydrogenase via S-nitrosylation in ethanol-exposed rat liver. FEBS Lett 2007;581:3967–72.
[66] Tamarit J, Cabiscol E, Ros J. Identification of the major oxidatively damaged proteins in *Escherichia coli* cells exposed to oxidative stress. J Biol Chem 1998;273:3027–32.